British Geological Survey
Natural Environment Research Council

BGS Commissioned Report CR/01/064N (released 06/05/08)

Multicomponent seismic monitoring of CO_2 gas cloud in the Utsira Sand: A feasibility study

Saline Aquifer CO_2 Storage Phase 2 (SACS2)
Work Area 5 (Geophysics) – Feasibility of multicomponent seismic acquisition
(Contract Number: T-124.167-02)

Enru Liu, Xiang Yang Li and Andy Chadwick

British Geological Survey,

Murchison House, West Mains Road,

Edinburgh EH9 3LA, United Kingdom

Tel. 0131 650 0362; Fax. 0131 667 1877

Email. E.Liu@bgs.ac.uk

This page is blank

Contents

Page

List of Figures

List of Tables

Executive summary

This document is part of the second phase of the Saline Aquifer CO_2 Storage (SACS2) project. It describes the results of Task 5.6 of Work Area 5 (Geophysics): Feasibility of multicomponent data acquisition. The aim of this Task is to evaluate the feasibility of multicomponent seismic data for monitoring the development and movement of the CO_2 bubble during CO_2 injection into the Utsira Sand at the Sleipner Field, North Sea.

For safety, stability and environmental considerations, it is necessary to know exactly where the injected CO_2 separated from natural gas will move, thus monitoring the CO_2 bubble development and movement in the underground reservoir is crucial for the success of the SACS2 project. Experience learnt from dynamic reservoir monitoring during fluid injection into reservoirs for enhanced oil recovery has indicated that the two key reservoir properties that are likely to change are fluid saturation and pore fluid pressure. These changes are observable in seismic data, and can be quantitatively predicted from time-lapse or 4D seismic surveys. However, it is of great interest to distinguish the effects of saturation and pore pressure in time-lapse seismic signals in order to monitor fluid movements and also to possibly identify unswept zones in reservoirs. In this report, we argue, using laboratory and field data examples, together with theoretical modelling, that conventional *P*-wave seismic data can be reliably used to estimate changes in fluid saturation, but provide little information about changes in pore pressure. Shear-waves (*S*-waves), on the other hand, though not as sensitive to fluid saturation as *P*-waves, are very sensitive to changes in pore pressure. We advocate that the combination of *P*- and *S*-wave data can be used to effectively differentiate fluid saturation and pore pressure. The information that shear-wave data can provide about fractures and the direction of fluid flow pathways is also very valuable. This is where the multicomponent time-lapse seismic monitoring (MC-TLSM) technology can play a significant part in monitoring the dynamic behaviour of the CO_2 aquifer at the Sleipner Field during large-scale injection of $CO_{2.}$

MC-TLSM is not only technically viable, but also cost effective in the long term. The physical basis of the technology is given in Section 4. In Section 5, we use four field examples taken from applications to the oil/gas reservoirs (as analogues to CO_2 injection at the Sleipner) to show the benefits of this technology primarily based on information provided by shear-waves. We demonstrate that MC-TLSM can play a major role in the following:

- Lithology and fluid prediction
  - Lithology discrimination
  - *Fluid verification/mapping and fluid discrimination*
  - *Pore pressure prediction*
  - *Fracture and stress state identification and characterisation*

- Improved imaging
  - *Structural imaging through gas cloud, chimney, etc.*
  - Imaging beneath high velocity layers
  - Depth determination

MC-TLSM also allows us to determine V_p/V_s which leads to Poisson's ratio, both for the caprock and for the reservoir sand, helping to constrain the elastic properties of these units. In the former case this information will help to evaluate sealing characteristics of the caprock. In the latter case it will help to constrain the Gassman equations which are being used to interpret the velocity pushdown of the bubble in terms of CO_2 volumes. We believe that at least the four highlighted items above (in *italics*) are related to the CO_2 disposal programme at the Sleipner Field. We conclude that (see Section 8):

☞ Sleipner Field is ideal for MC-TLSM, and the Utsira sand formation satisfies all criteria to be a 'good' candidate for such monitoring.

☞ Multicomponent TLSM provides a cost effective way of differentiating changes in fluid saturation and pore pressure that are likely to occur when a large amount of CO_2 gas is injected.

☞ Multicomponent TLSM technology has successfully been used in many oil/gas reservoirs in the North Sea and around the world, and the technology has matured. We now have all the hardware to acquire MC data and the software to quantitatively interpret the data.

The following are possible acquisition methods that could be used at Sleipner (Section 7).

1) *3D marine streamer survey (See Section 7)*. This is the cheapest option. In this we would look for *P*-wave AVO anomalies both laterally and azimuthally. The information provided by *P*-wave AVO can pinpoint areas with CO_2 concentration and the CO_2 front. The British Geological Survey, through the industry-funded Edinburgh Anisotropy Project, has developed advanced techniques to perform azimuthal attribute analysis of 3D *P*-wave data for estimation of fracture orientation and spatial distribution of fracture intensity (see Section 6). Analysis of 20 km^2 of typical 3D data would cost around \$20k to \$30k.

2) *3D OBC survey*. This technology is advancing very fast in the industry. Marine 4C seismology is the technology that places 4-components sensors (one-component hydrophone plus three-component geophones). The examples in Section 5 provide some good indications as how 4C OBC data can be used. Processing software of OBC 4C data are available and some are under development. A typical multicomponent OBC acquisition (say 20 km^2) would cost in the order of \$600k to \$750k, and processing cost would add another \$100k.

3) *Permanent reservoir monitoring system.* This is basically the same as (2), but a permanent reservoir monitoring system (PRMS) is installed in the monitoring site. The advantage with PRMS is the good repeatability. PRMS may sound expensive, but the incremental cost of future data acquisitions using PRMS should be lower as number of surveys increases.

We are confident that integration of dynamic information from time-lapse seismic with the other reservoir engineering data is vital for interpretation of the results. Considering the benefits and long term cost, we suggest that a permanent reservoir monitoring system using recently developed OBC technology offers both technologically viable and cost effective method at Sleipner.

1. Introduction

Large-scale storage of CO_2 in the subsurface is an unprecedented enterprise. It is therefore crucial to monitor the process carefully. The major task of monitoring is to record and control the stability of the reservoir and to observe the development of the expanding CO_2 bubble. A way to visualise the development of the CO_2 bubble is by performing seismic surveys across the storage site. The behaviour of a CO_2 bubble in an underground reservoir is in many ways analogous to the bubble of natural gas in a gas storage scheme. Extensive experience learnt from characterisation of gas reservoirs in the oil/gas industry has proved that the presence of natural gas in the pore spaces of a reservoir can be detected by seismic methods. To monitor the movement of CO_2 in the underground, the time-lapse (or 4D or repeated 3D) seismic survey is a natural choice. This report provides a feasibility study about monitoring injected CO_2 movement by innovative multicomponent seismic methods, which have attracted great interest in the oil/gas industry in recent years.

Time lapse seismic monitoring (TLSM) depends on injection-related changes in the acoustic velocity and density of the reservoir rocks. In its application to reservoir monitoring in oil/gas fields, TLSM technology can add value by helping to locate zones of depletion and to infer by-passed hydrocarbons, and by detecting significant reservoir features such as gas-cap expansion or water encroachment. The scientific basis for this technology can be considered generally sound. The 4D survey has been shown to fulfil the basic objective of detecting fluid movements for a variety of reservoir stimulation conditions including steam, CO_2 and water injection for a wide variety of geological environments (Wang 1997). Most potential monitoring applications rely on saturation changes that occur as native fluid in a reservoir is displaced by injected gas. The saturation changes dominantly affect the *P*-wave velocity of the reservoir because the compressional modulus of the rock is related to both the compressibility of the rock matrix and the compressibility of the reservoir fluids. Gassmann's (1955) equation is commonly used to predict the changes in *P*-wave velocity. The prediction indicates that the velocity sensitivity to fluid properties is greatest in unconsolidated (highly porous) rocks where the rock framework is highly compressible. Consolidated rocks, with lower frame compressibility, are generally less sensitive to changes in fluid properties. This suggests that time-lapse seismic monitoring is at best applicable to soft formation. Recent theoretical investigations predict that Gassmann's equation provides a low frequency limit to saturation-induced velocity change, but permeability heterogeneity can cause significant velocity increases as a function of frequency within the seismic band.

Before TLSM technology is applied we need answers to such questions as '*is the reservoir feasible for time lapse seismic monitoring?*' and '*what is the physical basis for such survey?*'. This report attempts to answer them. We review the latest development and application of marine multicomponent seismic, and suggest that the physical basis for time-lapse seismic monitoring of the CO_2 injection in the Utsira formation in the Sleipner Field is very strong. We argue that fluid saturation as well as pore fluid pressure changes that are likely to occur will produce an observable multicomponent 4D signature. As inspired by the work of Angerer (2001), we suggest that the shear-waves are more sensitive to detecting and monitoring dynamic attributes of the reservoir than *P*-waves, however, *P*- and *S*-waves together can be used to differentiate effects of fluid saturation and pore pressure. In addition, shear-wave data provide information related to velocity anisotropy, variation in pore pressure that can affect the percentage of open fractures and low aspect ratio pore structure, which will affect the degree of shear-wave splitting. Multicomponent seismic data can thus assist in separating effective stress changes from actual fluid property change. Traditionally, in the oil and gas industries, *P*-wave AVO (amplitude variation with offset) has been accepted as a 'standard' method for the detection of natural gas. There are many successful examples. The idea is based on the fact that because of the changes in the velocity ratio between the *P*- and *S*-waves induced by the gas, an increase in amplitude with offset (AVO) occurs at the gas/rock boundary, which appears on the seismic records as bright spot. Studies have shown that even a small amount of gas can cause a detectable bright spot. Therefore this technique (*P*-wave AVO) is ideal for monitoring CO_2 saturation. Shear-waves (*S*-waves), though not sensitive to the presence of fluid, are sensitive to pore pressure and seismic anisotropy caused by the preferred alignment of rock heterogeneities such as pore spaces (giving the preferred flow direction).

This report is arranged as follows. In Section 2, we briefly describe the SACS2 project. In Section 3, we introduce the concept of multicomponent seismology. In the corresponding Appendix A, we give some background information about the concept of seismic anisotropy. In Section 4, we use experimental and theoretical results to demonstrate the sensitivity of some multicomponent seismic attributes to fluid saturation and pore pressure. We demonstrate that the multicomponent seismic attributes containing the traditional *P*-wave attributes as well new shear-wave attributes are sensitive to fluid saturation and pore pressure. In Section 5, we use four field examples to show that multicomponent time-lapse seismic monitoring (or MC-TLSM) (1) can help indiscriminating lithology and fluid saturation; (2) can provide good images in the presence of a gas cloud; and (3) can be effectively used to monitor the CO_2 injection and associated changes in pore pressure. This last example is taken from Angerer (2001), who shows that in low porosity rock, such as dolomite or anhydrite, the fluid saturation has a much larger effect on *P*-waves than on shear-waves (which is Gassmann's prediction), but the pore pressure has a larger effect on shear-waves than on *P*-waves. This has a profound implication for monitoring CO_2 injection. In rock with high porosity, such as sandstone, a different response will be expected. But the sensitivity of shear-wave to pore pressure is an important finding. This is consistent with the laboratory experiment results of Wang *et al.* (1998). We include a study of azimuthal *P*-wave attribute analysis in Section 6 to demonstrate that fracture information can be extracted from *P*-wave data if sufficient azimuthal coverage is available. In Section 7, data acquisition and associated cost issues will be discussed. We summarise the main findings of this feasibility study in Section 8.

2. The SACS2 Project: A brief description

Currently, CO_2 separated from natural gas produced at the Sleipner Field in the northern North Sea (Norwegian block 15/9) is being injected into a saline aquifer, some 800 to 1000 m beneath the northern North Sea. Injection started in 1996 and shall last for twenty years at annual rates of approximately one million metric tons of CO_2. An international research project, the Saline Aquifer CO_2 Storage (SACS) project, accompanies the ongoing injection. Its aims are

1) to determine the local and regional storage properties of the reservoir (the Utsira Sand) and its overlying seal, and to assess their suitability for CO_2 injection elsewhere;

2) to monitor the injected CO_2 by geophysical methods;

3) to simulate and predict the present and future CO_2 distribution by reservoir modelling; and

4) to develop a 'best-practice' handbook to guide future CO_2 injection projects.

This report attempts to address items (2) and (4) above. The SACS project involves European research teams funded by industry and the European Union Energy Programme and governments to model and monitor the progress of the CO_2 storage at the Sleipner Field. Initial findings from time-lapse *P*-wave seismic monitoring indicates that the CO_2 is behaving as predicted with good vertical distribution within the storage reservoir, and containment by the caprock. Although conventional *P*-wave data have been used to detect changes in fluid saturation for many years in the oil/gas industry, the use of *P*-wave data alone render it difficult to distinguish the effects of saturation and pore pressure. Multicomponent seismology not only provides more attributes for analysis, but these attributes are particularly sensitive to pore pressure changes, which are likely to occur when a large amount of CO_2 is injected into the Utsira Sand.

3. Multicomponent seismology

Over the past two decades, shear-wave data have been used in oil/gas industry to evaluate fractured reservoirs in the search for hydrocarbon. Multicomponent data have been acquired in many areas for shear-wave studies. Field examples that demonstrate the significance of multicomponent seismology were given by Li (1997); Li and Mueller (1997); Liu *et al.* (1991); MacBeth (1995); Winterstein and Meadows (1991), etc. The basic concept is described in Appendix A, and the idea is based on the phenomenon of shear-wave splitting or birefringence (similar to the birefringence of light in crystal). A shear-wave will split into two waves travelling with different speeds with orthogonal polarisations (Figure 3.1) when entering an anisotropic medium containing aligned vertical fractures. For near-vertical propagation, the fast split shear-wave polarises parallel to the fracture strike, and the slow wave polarises nearly orthogonal to the fast wave (Figure 3.1). The time delay between two split shear-waves is proportional to the number density or intensity of fractures. Thus, in theory, one can obtain the fracture information of the underlying medium from shear-wave data recorded on the surface or in borehole.

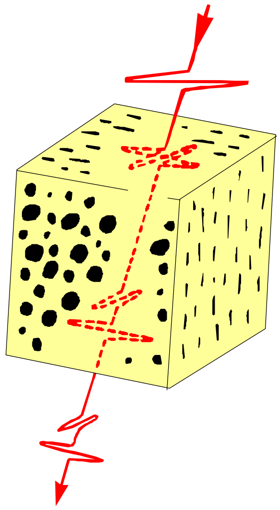

Figure 3.1 Schematic diagram showing the shear-wave splitting phenomenon, i.e. a shear-wave entering into an anisotropic rock will split into two orthogonal polarised waves.

With different configurations of sources and receivers, up to nine-component data (so-called full-wave data) can be recorded consisting of three polarised sources and three polarised geophones (Figure 3.2). Ideally, a full nine-component geometry is needed to describe the vector wavefield accurately. However, in practice, to minimise the cost of acquisition, several configurations of sources and receivers have been used depending on the purpose of the surveys (See Li and Mueller 1997).

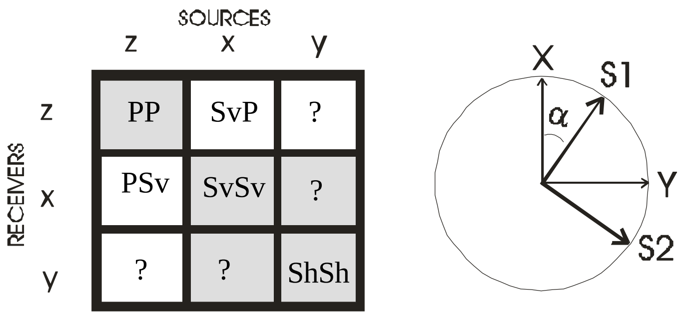

Figure 3.2 Data matrix for a full nine-component recording geometry. There are three orthogonal sources represented by the columns, and three orthogonal receivers by the rows. The shaded area represents the conventional five-component geometry used in VSP and surface data processing.

There are many successful examples (Li 1997; Li and Mueller 1997; Liu *et al.* 1991; MacBeth 1995; Winterstein and Meadows 1991). The usefulness of multicomponent seismic data was tested at the Conoco borehole test site, Oklahoma, USA. Horne (1995) found that the results obtained from a multi-azimuthal VSP from this site show that the shear-wave splitting results correlate very well with the lithology and permeability measurements derived from core data (Figure 3.3). Some of these zones have also been observed to correspond to considerable fluid loss during drilling which have been attributed to large open fractures.

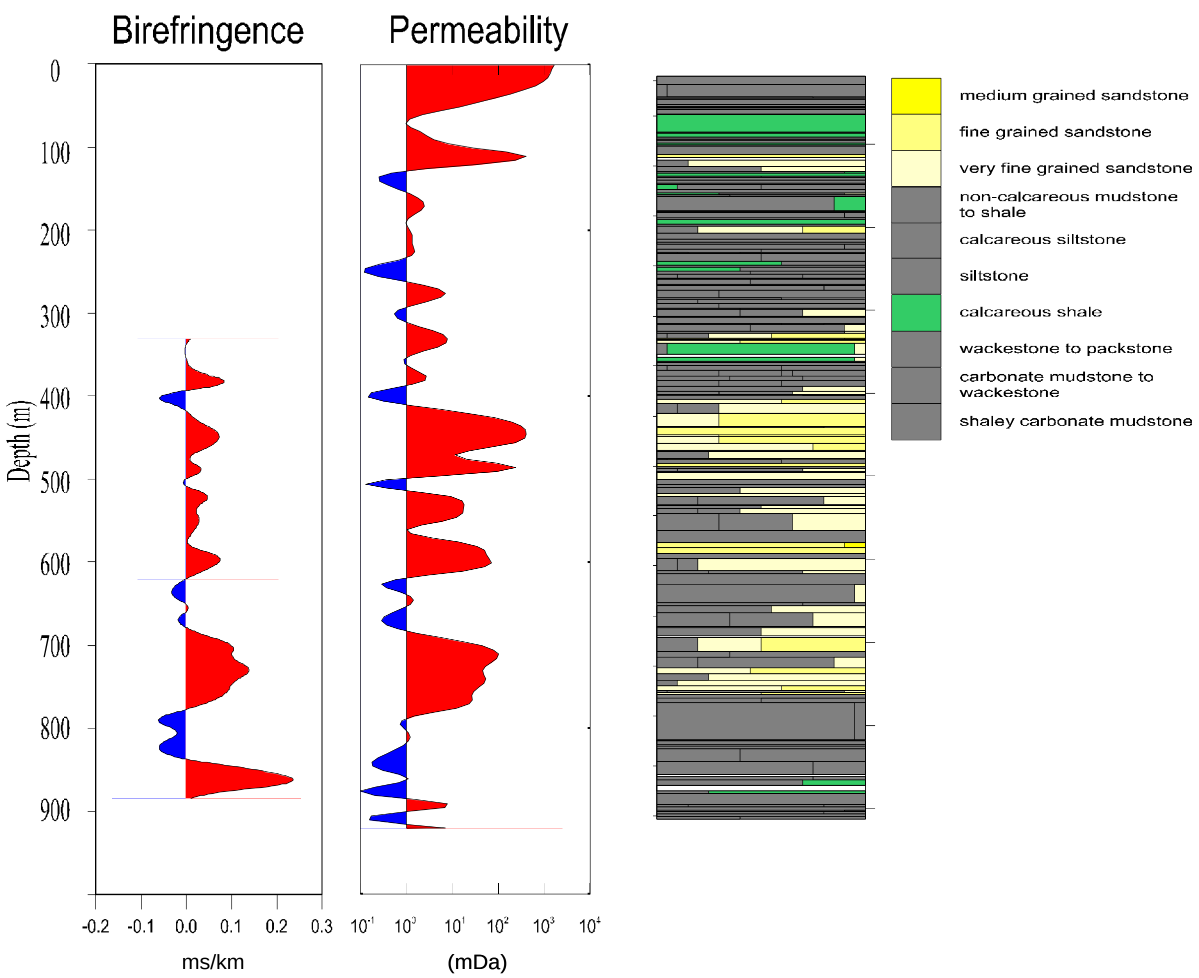

Figure 3.3 A comparison of the shear-wave splitting measurements with lithology and core measurements of permeability (after Horne, 1995).

However, because shear-waves do not propagate through water, the concept described above cannot be applied in offshore. A practical approach is to utilise *P*- to *S*-converted waves. Since the autumn of 1996, marine multicomponent seismology has become an important service provided by the geophysical industry. The essence of this technology is to record shear-waves on the seafloor with sensor packages containing hydrophones and three-component geophones (4-component or 4C) (Figure 3.4). New processing algorithms have to be developed to properly process these data. BGS, through the industry-funded Edinburgh Anisotropy Project (EAP), has been developing advanced techniques to process and interpret OBC 4C data. In Section 5, some examples will be used to demonstrate the values of OBC 4C seismology.

Recently, industry-scale multicomponent acquisition has been used for time-lapse reservoir surveying or monitoring purposes using permanently installed ocean-bottom or down-hole sensors. Over 100 marine OBC surveys have been acquired during the period of 1996 to 1999 (Caldwell 1999). The motivation for these offshore multicomponent studies is the ability of converted waves to see through gas clouds or image subtle *P*-wave impedance targets. Recently OBC 4C data have provided valuable information about lithology discrimination and fluid prediction. In this area, multicomponent time-lapse surveys have the potential of contributing much added information to the map of reservoir changes.

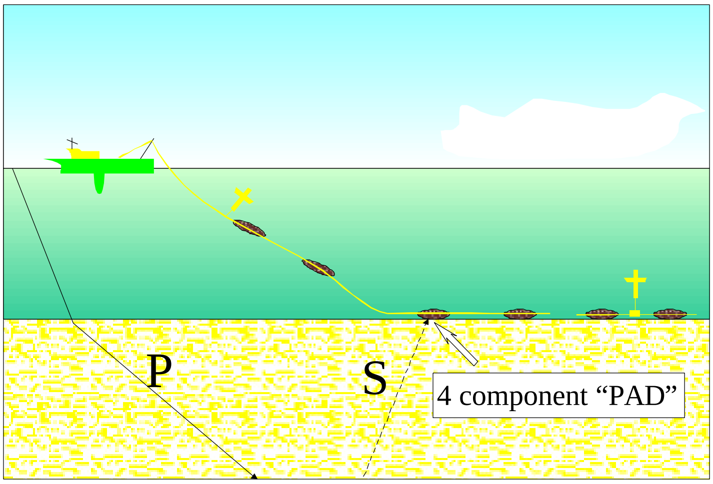

Figure 3.4 Schematic diagram showing converted shear-waves can be recorded in 4C data on the seabed.

4. Multicomponent seismic monitoring: The physical basis

Time-lapse seismic has increasingly been used to monitor subsurface fluid distributions, pressure changes and fluid fronts/movements in producing hydrocarbon reservoirs (Wang 1997). With seismic reservoir monitoring, it is essential to know how seismic response is influenced by changes in relevant reservoir parameters. Nur (1989) listed at least 20 rock parameters that may change during oil/gas extraction or during fluid (water, gas, steam, CO_2, etc.) injection. However, the most important and fundamental parameters are expected to be fluid saturation and pore pressure. Other factors that affect seismic properties include stress, temperature, fluid types, and frequency. Table 4.1 lists some of the most important reservoir properties and summarises the main reservoir parameters that may change during CO_2 injection. It also includes a comparison of the conventional and multicomponent seismic attributes. Wang (1997); Wang *et al.* (1998) have carried out extensive laboratory experiments to study the variation of changing rock properties affecting seismic properties. The dynamic response of cracked and porous rock has been studied theoretically by Hudson (2000); Chapman (2001); and Pointer *et al.* (2000). These dynamic rock-fluid models are capable of being easily calibrated using data available at the wells, and are consistent with petrophysical data, and ultimately have the ability to scale both up and down.

Table 4.1 Rock properties and seismic attributes

Reservoir properties	**Conventional *P*-waves seismic attributes**	**Multicomponent seismic attributes**
• Porosity • Density • Saturation • Fluid type • Permeability • Pore pressure • Temperature	• Seismic velocity (V_p) • Travel time (t_p) • Acoustic impedance • Amplitude/attenuation • AVO response • Azimuthal response	• Seismic velocity (V_p, V_s) • Travel time (t_p, t_s) • V_p/V_s ratio • Acoustic impedance • Elastic impedance • Amplitude/attenuation (*P*, *S*) • AVO response (*P* and *PS*) • Azimuthal response • Shear-wave splitting • Shear-wave polarisation

In this Section, we summarise some of the results with emphasis on the effect of fluid saturation and pore pressure. We show that the physical properties of rocks are sensitive to both fluid saturation and pore pressure, which have significant effects on measurable anisotropic parameters and AVO response. We emphasise the fundamental role that shear-waves play in determining rock physical properties. However, our study shows that it is difficult to distinguish the effects of fluid saturation and pore pressure from the *P*-wave analysis alone, and that joint analysis of both *P*- and *S*-waves is necessary.

4.1 Shear-wave information is necessary for lithology prediction

It has been known for a long time that the measurement of shear-wave velocity (V_s) (and Poisson's ratio) is important for understanding reservoir properties (Figure 4.1). V_s is required for rock strength analysis to determine fracture propagation and formation breakdown characteristics. V_s also provides improved porosity prediction as it largely unaffected by fluid types. It is also becoming important for enhanced geophysical interpretation such as AVO analysis and acoustic/elastic impedance inversion. Because the value of shear-wave velocity data is only now being realised, coupled with the high cost of acquisition, there is a limited amount of shear-wave information available from the North Sea. One way of predicting shear-wave velocity is from existing log data and there are several proposed techniques (such as Xu and White 1995; Yan *et al.* 2001). When such logs are unavailable, shear-wave information can only be obtained through multicomponent seismic data. Recently Connolly (1999) introduced the concept of elastic impedance (EI) which is basically the extension of the acoustic impedance (AI) for non-normal incidence angles. Very recently the

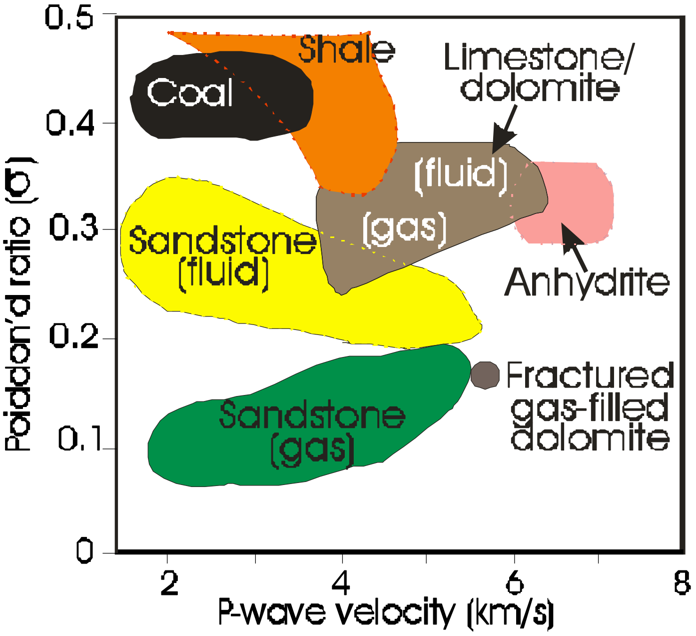

Figure 4.1 Lithology classification based on *P*-wave velocity (V_p) and Poisson's ratio (σ) (V_p/V_s is required to obtain σ).

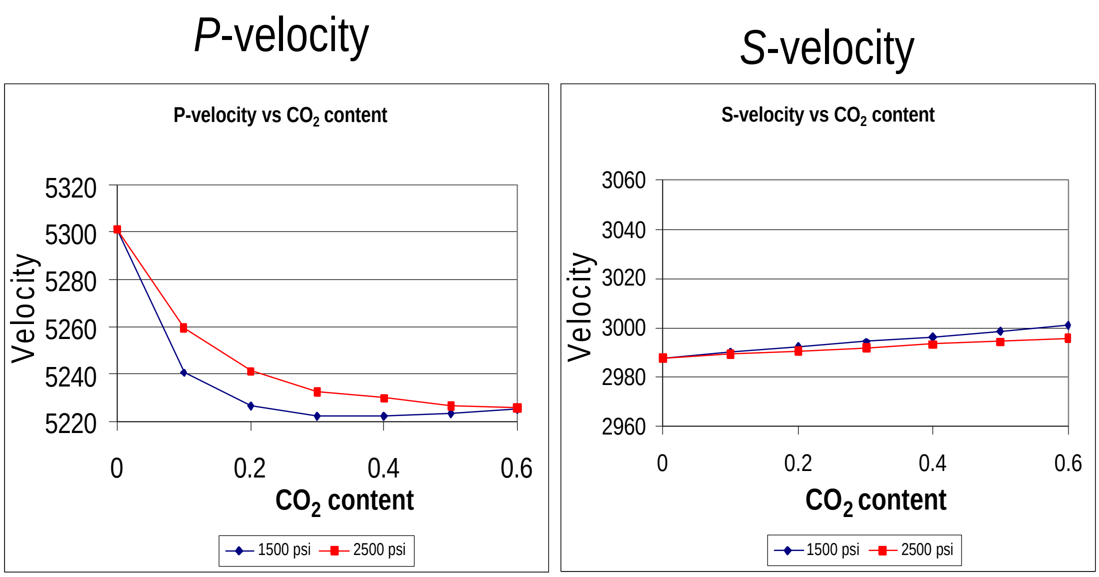

Figure 4.2. *P*- and *S*-wave velocities of the San Andres formation (dolomite) for varying CO_2 content and for two pore fluid pressure (after Angerer, 2001).

corresponding shear elastic impedance (SEI) is also being introduced to industry by Duffaut *et al.* (2000). Both EI and SEI, which require shear-wave information, may be used as indicators of lithology and fluid saturation. Stearn *et al.* (2001) demonstrated that inversion of the converted shear-wave (*PS*) data to get elastic impedance greatly aided the interpretation of the data and allowed estimates of sand thickness. They emphasised that acquiring multicomponent seismic data was the key step in reducing development risk.

4.2 Shear-wave is not sensitive to fluids?

In rock physics the porosity of a rock is commonly divided into two categories, crack-like porosity and circular or equant (matrix) porosity (Thomsen 1995; Hudson *et al.* 1996); known as clay and sand porosity or also soft and hard porosity (Xu and White 1995). The difference between these two types of porosity is that the cracks are sensitive to pressure changes, as they are soft and can therefore open and close with varying pressures. Equant porosity does not alter its shape when pressures change. It is therefore only affected by saturation changes. Crack-like porosity is sensitive to both saturation and pressure changes.

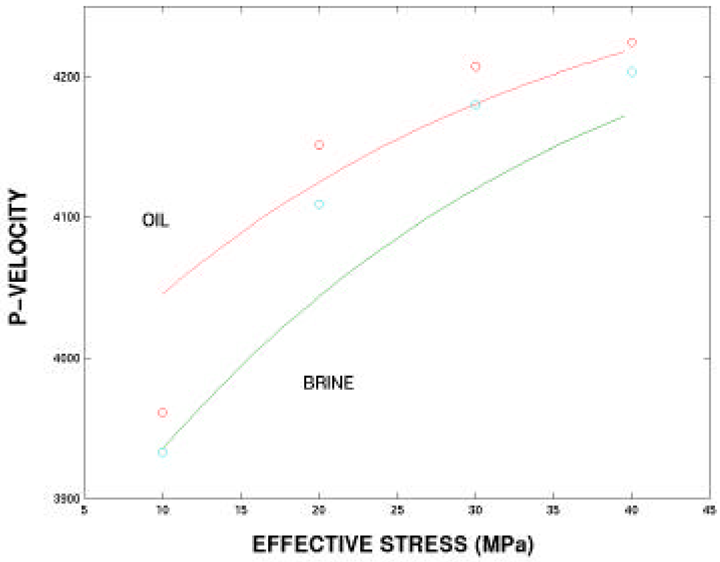

Figure 4.3 Ultrasonic *P*-wave velocity measurements for oil and brine saturations for different values of effective stress. Solid lines are theoretical curves using the model described by Chapman (2001).

Gassmann's (1951) theory, which is normally used for fluid substitution, only considers equant or matrix porosity. Gassmann's theory predicts that the shear modulus is independent of fluid saturation. Figure 4.2 shows the variation of *P*- and shear-wave velocities of dolomite for varying CO_2 content and two pore pressures (Angerer 2001). The dolomite with up to 20% anhydrite has a low porosity of 12%. The *P*-wave velocity decreases with increasing CO_2 content, significantly so for small amounts of CO_2. However, shear-wave velocity shows more or less a constant variation with increasing CO_2 content, and the small shear-wave velocity variation is attributed to the decreasing of density with increasing CO_2 content. This is consistent with the prediction of Gassmann's theory. Figures 4.3 and 4.4 show the variation of measured *P*- and *S*-wave velocities at ultrasonic frequency with effective stress for a sandstone sample (Chapman 2001). This sandstone sample has a porosity of about 22%. We can see that both *P*- and *S*-wave velocities show a remarkable dependence with effective stress and saturation. When the effective stress is increased from 10MPa to 40MPa, the change in the *S*-wave velocity is about 12% as compared with 6% change in the *P*-wave velocity. Chapman (2001) argues that Gassman's theory seriously underestimates the effects of fluid saturation, and the dispersion. He found that it is necessary to include the effects of crack-like porosity as well as equant (matrix porosity). The continuous curves (Figures 4.3 and 4.4) are the best match using the newly developed dynamic poroelastic theory by Chapman (2001).

Since it is now well known that shear-wave data is much more sensitive to crack-like porosity, it is misguided simply to assume that shear-wave is not sensitive to fluids. For low porosity, low permeability rocks, it is true that *P*-wave velocity is more sensitive to saturation than shear-waves. For high porosity, high permeability rocks however, such statement can be incorrect since density has a strong dependence on porosity, thus leading to variation of shear-wave velocity with porosity. However, shear-waves are more sensitive to changes in pore pressure. The theory provided by Chapman (2001) is ideal for this purpose.

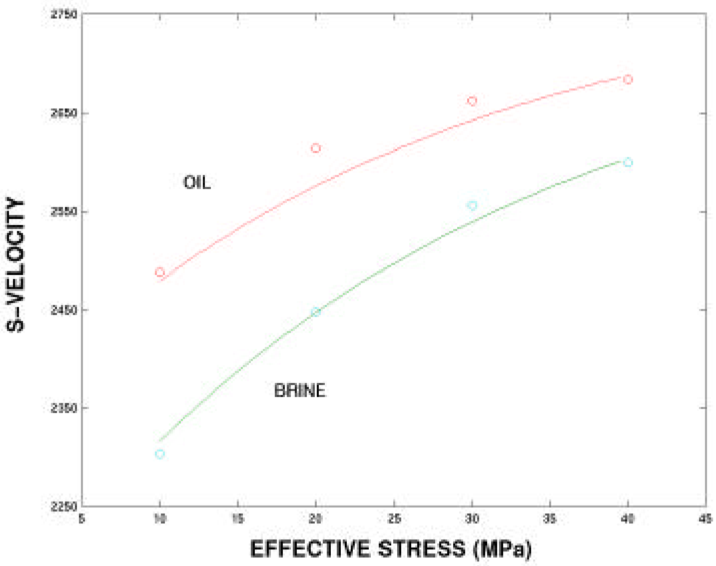

Figure 4.4 Ultrasonic *S*-wave velocity measurements for oil and brine saturations for different values of effective stress. Solid lines are theoretical curves using the model described by Chapman (2001).

4.3 The effects of gas/CO_2 injection

During CO_2 (or other gas) injection, two rock properties are likely to change. The first is a change in fluid saturation and the second is a change in pore fluid pressures. Figure 4.5 shows a schematic diagram on the effects of gas/CO_2 injection on *P*- and *S*-wave impedance. Figure 4.6 shows the similar plot to Figure 4.5, but calculated using the theory of Chapman (2001) for rock properties roughly comparable to the Utsira Sand (V_p = 3000m/s, V_s = 2000m/s, and porosity ϕ = 30%). When pore fluid is changed from water to CO_2, it is expected that the *P*-wave impedance will decrease, whereas pore pressure will increase. A similar feature is seen for *S*-waves, but the saturation will have a much smaller effect than for *P*-waves. Subsequently, we may argue that *P*-waves are sensitive to both the CO_2 saturation and pore pressure, but *S*-waves are particularly sensitive to the pore pressure increase. As a result, the combined *P*- and *S*-wave changes caused by the CO_2 injection may be used to separate CO_2 injected zones with pore pressure build-up from those regions without pore pressure build-up. Wang *et al.* (1998) carried out extensive laboratory experiments to demonstrate that the largest V_p and V_s changes caused by CO_2 injection are associated with high-porosity and high permeability rocks. In other words, CO_2 injection and pore pressure build-up affects V_p and V_s more in soft formation.

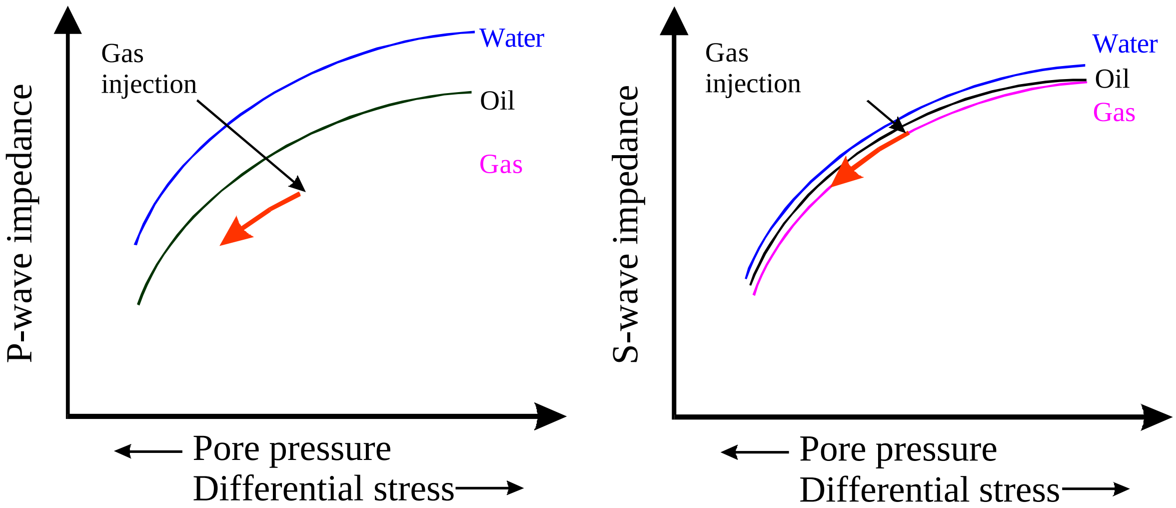

Figure 4.5 Schematic diagram showing the variation and *P*- and *S*-impedance with pore pressure and saturation during CO_2 injection.

4.4 Effects of stress and saturation on P- and S-wave anisotropy.

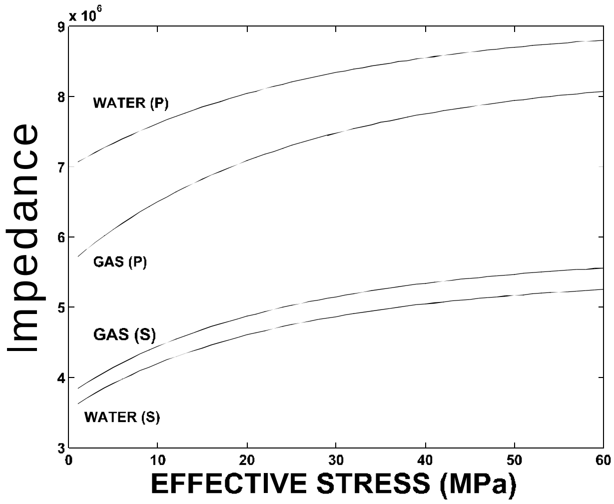

Figure 4.6 Variation of *P*- and *S*-impedance with effective stress for a rock with roughly comparable properties to the Utsira Sand.

Aligned cracks and pore space will be expected to introduce azimuthal anisotropy (Appendix A). Crampin (1990) has advocated the use of seismic anisotropy for reservoir monitoring. It is now common to measure the degree of anisotropy in terms of Thomsen's anisotropic parameters (Appendix A). Figure 4.7 shows the variation of Thomsen's two anisotropic parameters ε and γ with normalised pore pressure computed for different saturations (crack initial aspect ratio is 0.001). These two parameters measure the degree or percentage of *P*- and *S*-wave anisotropy, respectively. We can see that as pore pressure increases, which is equivalent to increase in the crack aspect ratio, both *P*-wave and *S*-wave anisotropy increases. The increase in shear-wave splitting parameters γ with increase in pore pressure is consistent with the field observation by Angerer (2001), who shows that significant change in time delay between split shear-waves was attributed as due to the increase in pore pressure after CO_2 injection in the Vacuum field (see Section 5). As normalised bulk modulus and shear-modulus of fracture-filling material increases from pure gas-filled cracks to water-filled, anisotropic parameters decrease. However, as expected the largest variation is ε (as *P*-waves are more sensitive to fracture filling properties). Guest *et al.* (1998) have observed that shear-wave splitting is significantly higher for gas-filled than for fluid-filled fractures, and their observation

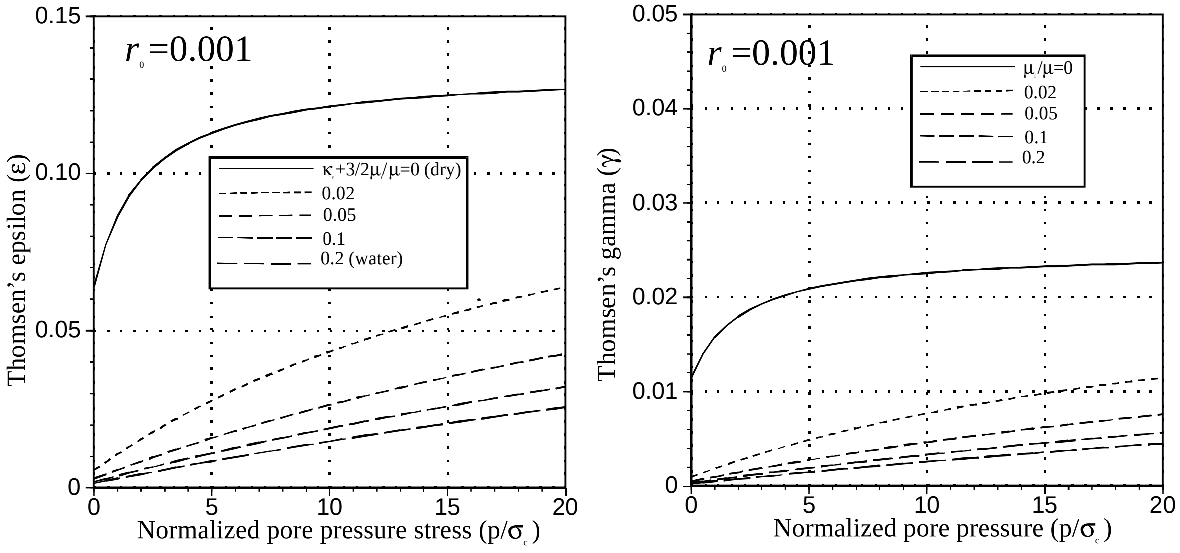

Figure 4.7 Showing changes in anisotropy (Thomsen's parameters) as a function of pressure changes (after Liu and Li, 2001).

is consistent with the results in Figure 4.7 if we introduce a small shear-modulus or viscosity in the fracture-infill.

4.5 Sensitivity of PP and PS-reflectivity to saturation and pore pressure

Another key seismic method is AVO (amplitude variation with offset) analysis. Figures 4.8 and 4.9 show the effects of fluid saturation and pore pressure on the plane *P*- and *S*-wave reflection coefficients (R_{PP} and R_{PS}, respectively) for shale overlying a fractured sandstone layer. The AVO curves are computed for the azimuth perpendicular to fracture orientation. For moderate angles of incidence the water-filled and gas-filled fractures begin to separate, with the reflection coefficient for dry fractures becoming increasingly large (Figure 4.9). A similar feature can be seen in Figure 4.8 for variation of pore pressure. Comparing Figures 4.8 and 4.9, we find that an increase in saturation (from gas to water, say) is equivalent to a decrease in pore pressure in both the *P*- and *PS*-wave AVO response. This suggests that it will be difficult to distinguish between the effects of saturation and pore pressure from AVO data alone.

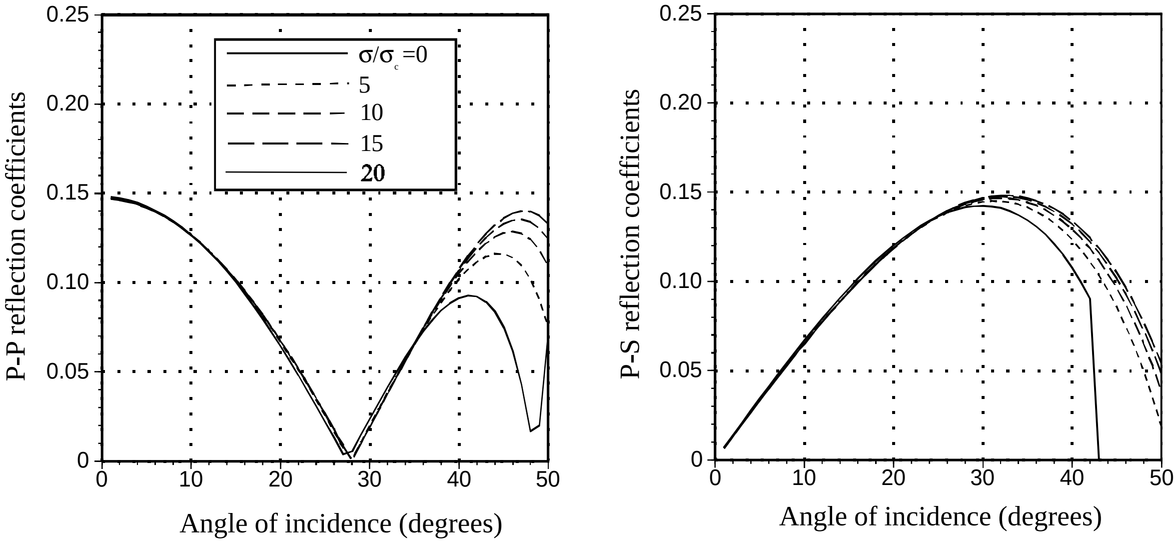

Figure 4.8. Variation of reflection coefficients R_{pp} and R_{ps} with normalised stress over a fractured reservoir (after Liu and Li, 2001).

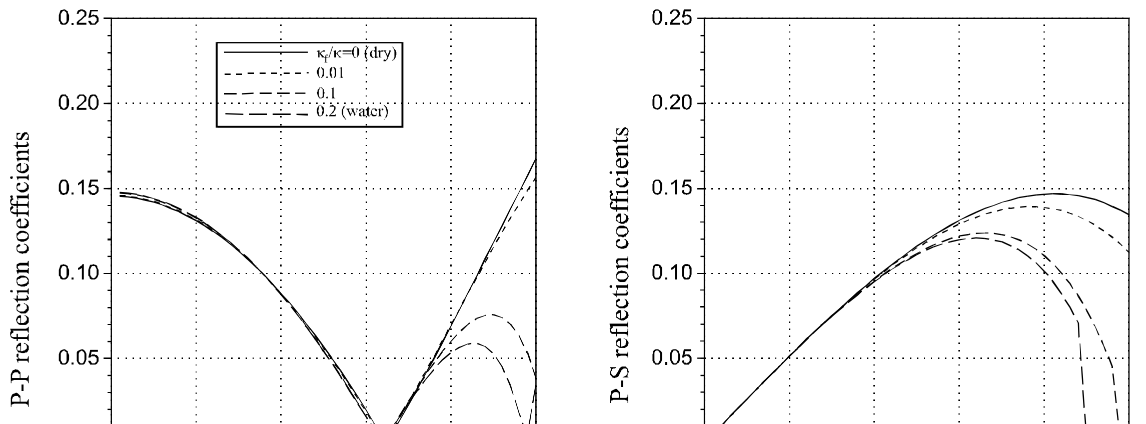

Figure 4.9. Variation of reflection coefficients R_{pp} and R_{ps} with saturation over a fractured with line azimuth perpendicular to the fracture strike (after Liu and Li, 2001).

5. Multicomponent seismic monitoring: The examples

It has been proved by many laboratory measurements and theoretical predictions (as well as in the last Section) that the multicomponent seismic monitoring can provide valuable information about a reservoir interval ad associated layers. The use of multicomponent seismics has been very successful, particularly in the following areas:

- Lithology and fluid prediction
  - Lithology discrimination (sand and shale)
  - Fluid verification/mapping and fluid discrimination
  - Fracture and stress state identification and characterisation

- Improved imaging
  - Structural imaging through gas cloud, chimney, etc.
  - Imaging beneath high velocity layers
  - Depth determination

For each of the listed topics above, there are many successful examples (see Caldwell 1999). In this Section, we shall demonstrate the value of multicomponent seismics for monitoring the dynamic response of reservoirs. We shall give four examples that are relevant to the CO_2 disposal environment. The first example shows that the lithology and fluid indicator V_p/V_s can be effectively estimated from converted shear-wave data. The second example shows that converted waves from OBC 4C data can help discriminate internal reservoir structures. The third example shows the classic case of using converted shear-waves to improve the imaging in the presence of gas clouds. The last example demonstrates the response of 3D multicomponent shear-wave data to CO_2 injection in the Vacuum field in New Mexico. In addition, we have used downhole multicomponent seismic data to monitor the growth of a hydraulic fracture (Liu *et al.* 1997), and also to locate a shallow high permeability zone or fracture (Majer *et al.* 1996).

5.1 Estimation of V_p/V_s ratio from converted shear-wave data (North Sea)

Poisson's ratio is completely determined by the V_p/V_s ratio, and both are important quantities for lithology prediction and fluid substitution for reservoir modelling and simulation as showed in Figure 4.1 (see also references by Tatham 1982; Robertson 1987; Iverson et al. 1989, and among others). For marine seismic data, AVO modelling has conventionally been the only practical method of obtaining *S*-wave information. The emergence of marine 4C technology opens new opportunities to obtain *S*-wave information from *P-SV* converted waves (*PS*-waves) recorded at the seabed. The V_p/V_s spectrum can be obtained from the converted shear-wave data if the *P*-wave velocities are known. This allows the unique determination of the V_p/V_s ratio from multicomponent data (Li et al., 1999; Yuan et al. 1999). Figure 5.1 shows an example of the contour V_p/V_s ratio section for processing of the OBC data from a producing oil field in the North Sea. The technique for estimation of V_p/V_s is similar to the conventional velocity analysis for processing *P*-wave data, and Li et al. (1999) and Yuan et al. (1999) have shown that their technique is robust and very reliable.

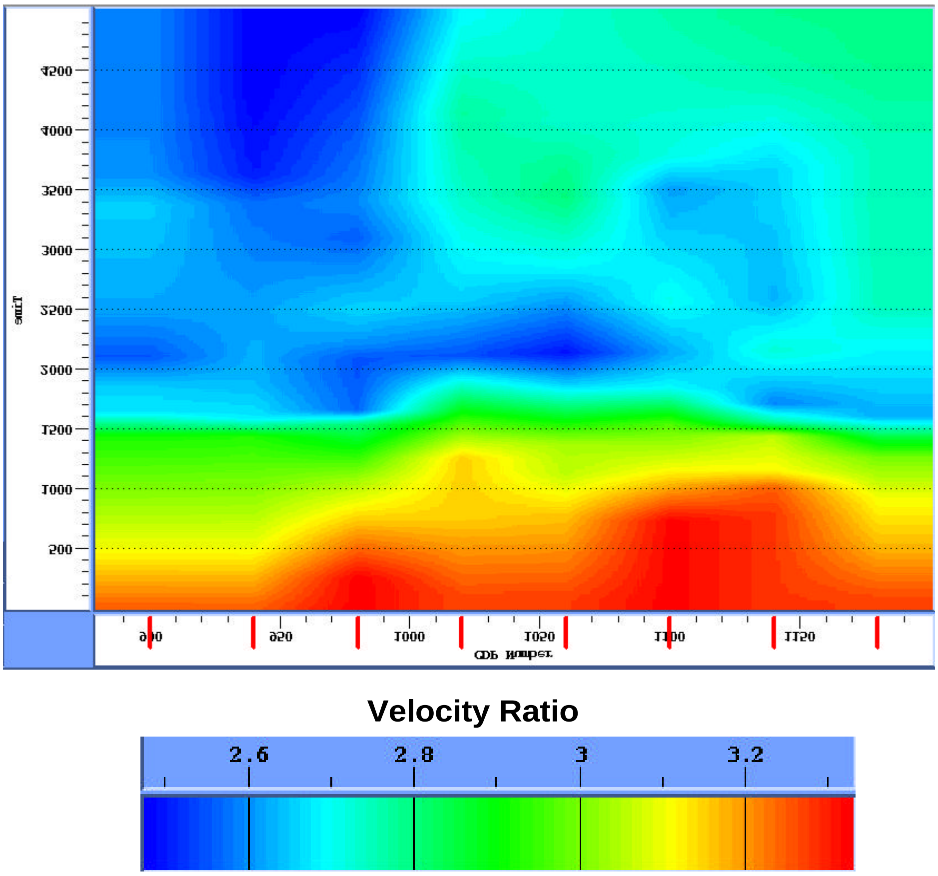

Figure 5.1 shows an example of the contour V_p/V_s ratio section for processing of the OBC data from a producing oil field in the North Sea data (after Li et al. 1999).

5.2 Using shear-waves to discriminate lithology (Alba Field, North Sea)

Converted shear-wave seismic data have been very useful in delineating stratigraphically equivalent reservoir sands. A famous example from the Alba field in the central North Sea (Hanson *et al.* 1999; MacLeod *et al.* 1999), is reproduced in Figure 5.2. The Alba field consists of high porosity, unconsolidated turbidite channel sands sealed by low permeability shales at an average sub-sea depth of 1900m. The challenge is to improve the seismic imagining at Alba to allow accurate placement of horizontal wells and better estimation of oil in place. Furthermore, prediction of water saturation ahead of well drilling is crucial. The aim is to use converted shear-waves to image low *P*-impedance reservoirs. The reservoir is an oil-filled sand where the *P*-wave impedance contrast between the top of the reservoir and the overlying rocks is essentially nil. The sonic and density data also indicate no changes in V_p at depth. The oil-water contact (OWC) is visible in both sections. But the sand channel is clearly visible in the converted wave section. The *PP*-section (Figure 5.2, left) clearly shows the OWC, while the *PS*-section (Figure 5.2, right) shows a different picture, which is interpreted as the internal structure of the reservoir related to stratigraphy variation. This can be clearly seen in Figure 5.3, where *P*- and *S*-log curves showing

OWC clearly seeing in the P-wave, but the S-wave shows a marked difference in lithology. MacLeod *et al.* (1999) conclude that the interpretation of the converted shear-waves is now a critical component of our understanding of the structure of the Alba reservoir, and is central to future well planning. This interpretation is the primary input for the construction of a new full-field reservoir model. Time lapse changes seen in the PS-wave data are changing our understanding of fluid flow and are impacting well placement.

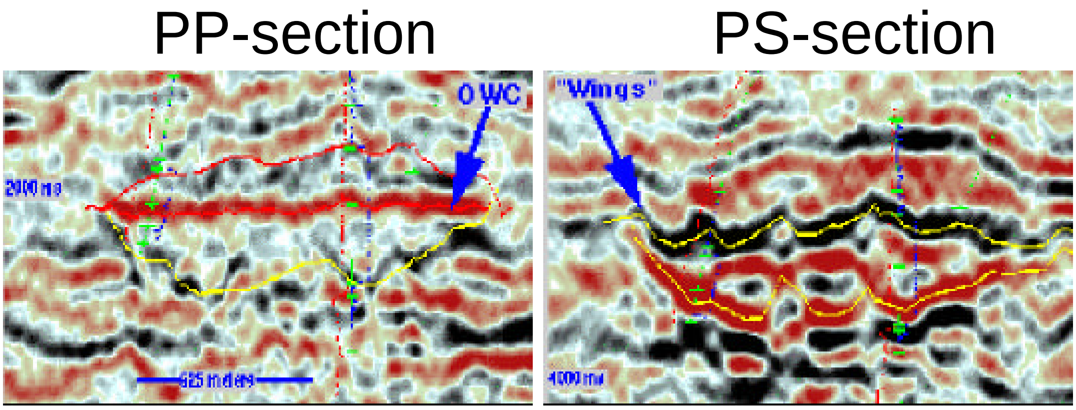

After Hanson et al (1999)

Figure 5.2 The data are from the Alba field in the North Sea. The left section is the *PP* data m and the right section is the *PS* section. The top of the reservoir is not visible in the *PP* data, but is very evident in the *PS* data (adapted from Hanson *et al.*, 1999).

Figure 5.3. Logs from the Alba field. V_p shows no change at the top of reservoir, but V_s does. However, the oil-water contact is clearly visible in the P-wave log (adapted from Hanson *et al.*, 1999; Macleod *et al.*, 1999).

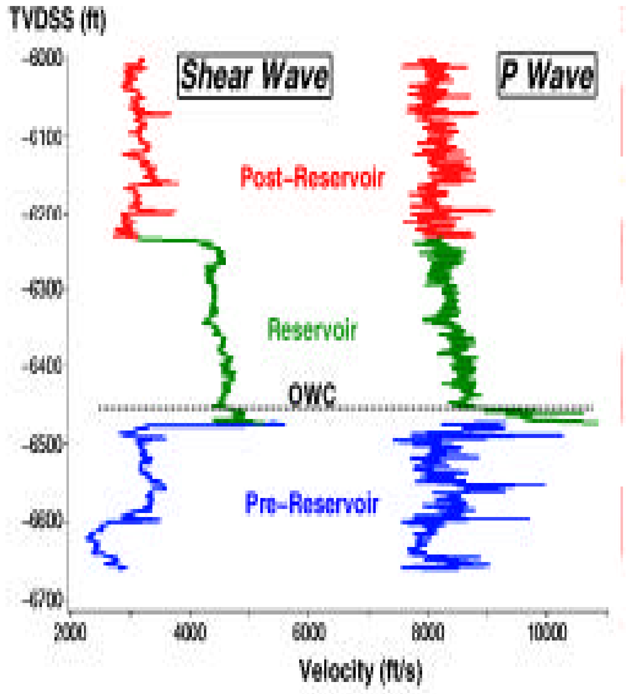

5.3 Imaging gas cloud using converted shear-waves (Valhall Field, North Sea)

Imaging of gas clouds and gas chimney using OBC converted waves has been successful in the North Sea, offshore Indonesia, offshore China, the Gulf of Mexico, and offshore West Africa. The Valhall reservoir of the North Sea is a classical example that cannot be well imaged by conventional *P*-wave techniques. Figure 5.4 (left) shows a 2D *P*-wave section extracted from a modern 3D *P*-wave volume, extending across the heart of the reservoir. The event at about 3000 ms on each side of this image is the top of the chalk reservoir; in the centre of the section the event is depressed in time by about 400 to 500 ms, and has low amplitude and coherency. Identification of faulting or other internal compartmentalisation of the reservoir is impossible to discern, so optimal production of this valuable resource is problematic. The classical interpretation of these effects is that, over geological time, gas has leaked from the reservoir into the overburden, in the zone above the reservoir. This gas, while present in uneconomic concentrations, has the effect of both lowering seismic velocities, and of increasing seismic attenuation, producing the effects described above. The physical explanation of this is that the compressible gas in the pore space disproportionately reduces the stiffness of the rock in compression, hence lowering its *P*-wave velocity. Also, at seismic frequencies, the dominant mechanism of *P*-wave attenuation is the ‘squirt’ of fluid within the pore space; this mechanism is enhanced if the pore fluid is compressible. These physical arguments also produce the prediction that these effects should not be present in a shear-wave study, since the compressibility of pore fluid is a second-order consideration with such waves. Thus the image obtained from converted shear-waves shows much clearer stratigraphical resolution beneath the gas cloud (Figure 5.4, right).

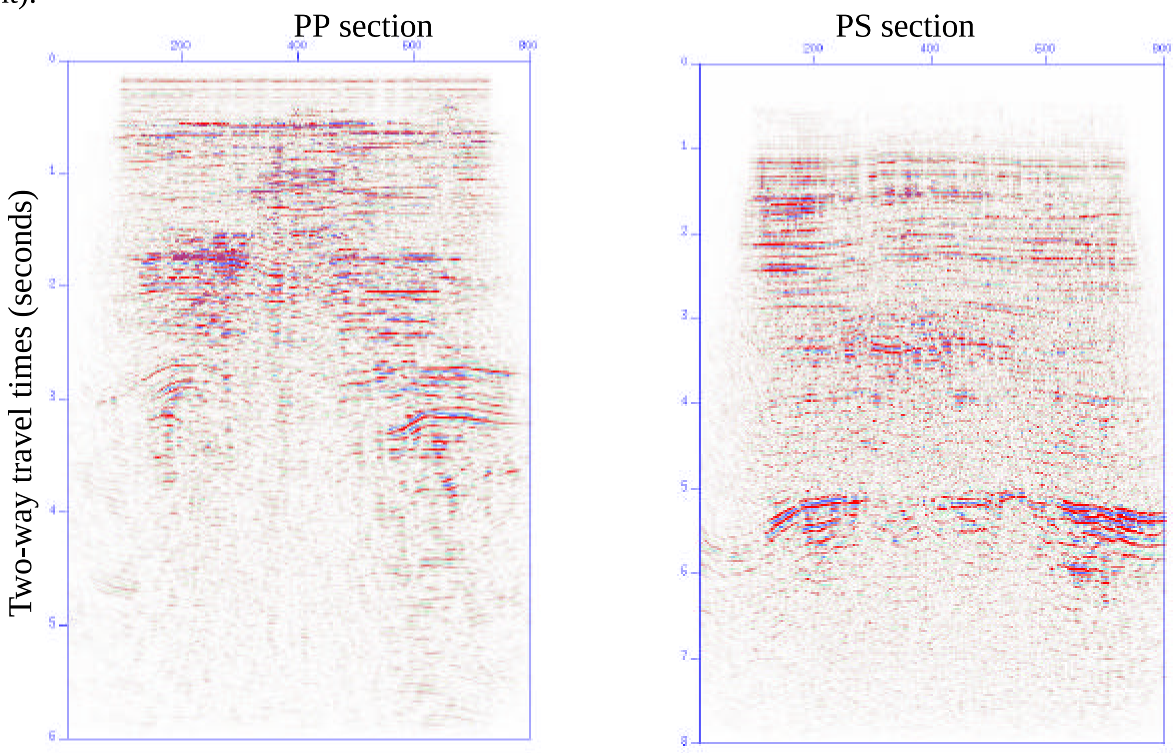

Figure 5.4. The *PP* imaging (left) and the *PS* imaging (right) shown in the figure are from the Valhall in the North Sea. The *PP* data are disrupted due to gas cloud. The *PS* data show the continuous layers across the whole section (after Dai and Li, 2001).

5.4 Monitoring dynamic reservoir response during CO_2 injection (Vacuum Field, New Mexico)

TheVacuum field, New Mexico, is a fractured dolomite. In 1995, over a period of two months, two nine-component seismic surveys were acquired by the Colorado School of Mines Reservoir Characterisation Project before and after a pilot EOR program of CO_2-injection, which significantly increased the reservoir pressures from 10.6MPa to 17MPa and altered the fluid composition (Angerer 2001; Angerer et al. 2001). After applying a processing sequence that aimed to preserve anisotropy and maximise repeatability, interval-time analysis of the reservoir interval shows a significant 10% change in shear-wave velocity anisotropy and 3% decrease in the *P*-interval velocities. A 1D model incorporating both saturation and pressure changes is matched to the data. The saturation changes have little effect on the seismic velocities (see Figure 4.2). The main cause for the time-lapse changes is the pore-fluid pressure increase which modifies crack aspect-ratios.

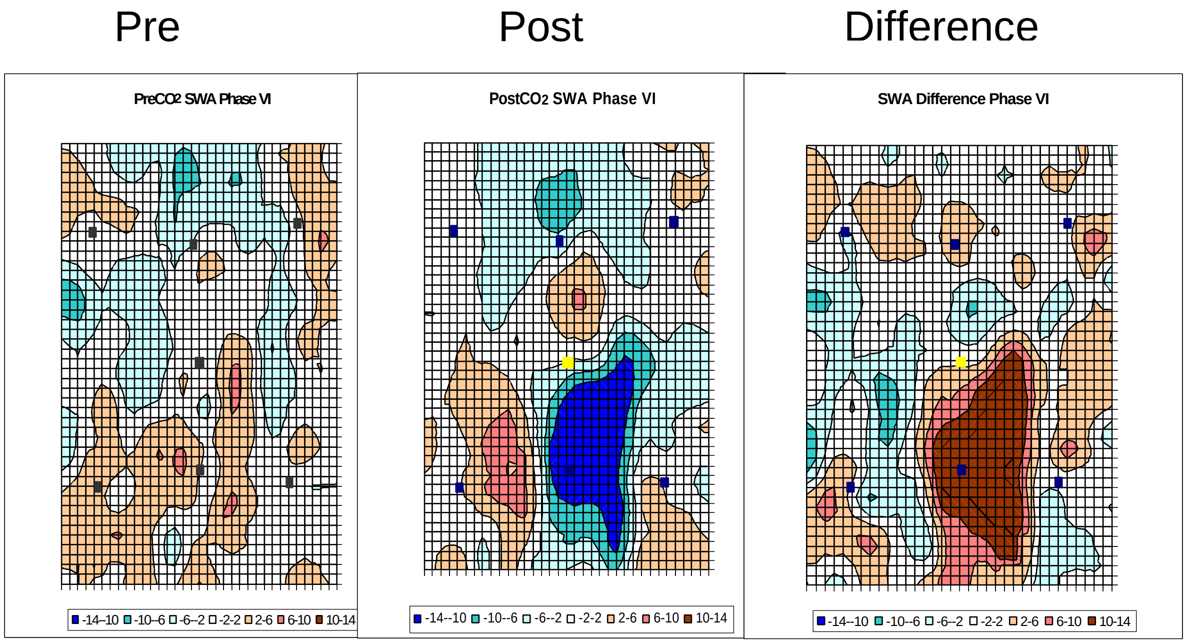

Figure 5.5 Plan view of shear-wave anisotropy (time delay) of the San Andres interval (dolomite) before and after CO_2 injection over a period of two months. Values are in percent The CO_2 (yellow) and water injection (blue) wells are indicated. Each grid point is one CMP location (after Angerer, 2001).

Angerer (2001) performed anisotropic analysis on the stacked data. The horizon picks provide interval travel times and time-delays of the split shear-waves, which are used to calculate the percentage of shear-wave velocity anisotropy as the normalised difference between the fast and the slow shear-wave velocities. Figure 5.5 shows the percentage time delays between the *S1* and the *S2* shear-wave components (percentage difference in shear-wave anisotropy) before and after injection. Before the injection, the shear-wave time delays lie mostly between ±2%, which means shear-wave splitting is small and lies just above the limits of resolution. After the CO_2 injection a zone with negative shear-wave splitting can be observed in Figure 5.5 to the south and east of the injection well. The average value of anisotropy in the anomalous zone is –8%. Peak values lie around –12%. Both shear-wave components decrease differentially after the injection, where the *S1* component decreases more than the *S2* component. This produces a "negative anisotropy" where the shear-wave polarised parallel to the maximum horizontal stress direction is slower than the perpendicularly polarised wave. A similar observation of a negative anisotropy (90°-flip in polarisation direction) was made in an over-pressurised reservoir by Crampin *et al.* (1996). The *P*-wave interval time difference plot (not shown here) shows a zone of velocity decrease to the south and east of the injection well, with an average velocity change in this zone of 2% with peak values of 5%. The zone to the NW of the injection well shows very little changes in *P*-wave velocities. From the interval-time analysis it can be concluded that the combined effects of CO_2-injection and increase in pore-fluid pressure are decreases in all wave velocities occurring mainly to the south and east of the injection well.

Figure 5.6 shows the resulting polarisation directions of the target interval for the pre-CO_2 and the post-CO_2 surveys. To the NW, the polarisation directions are in general more uniform and aligned parallel to the natural co-ordinate system. To the SE, the polarisations are very heterogeneous, especially in the pre-CO_2 survey. After injection there is better alignment in this quadrant. A possible explanation is that before CO_2-injection the reservoir may have been in a very heterogeneous condition as both production and water-injection processes had been in progress for decades. It is suggested that the significant pore-fluid pressure increase between the two surveys may have led to more homogeneously aligned polarisation directions in the whole area. There is no significant polarisation anomaly in the area of the identified time-delay changes. The absolute value of shear-wave velocity anisotropy changes from an average of 2.2% to -8% after the high-pressure CO_2-injection in the reservoir to the S and SE of the injection well (the negative anisotropy represents a 90°-flip in the polarisation of the faster split shear-wave). This zone correlates with zones of low seismic coherency, indicating the presence of faults and fractures. After the CO_2-injection the shear-wave polarities are reversed as the shear-wave parallel to the maximum stress direction becomes the slow wave and the transverse shear-wave becomes the fast wave. This 90°-flip is characteristic of the response of shear-waves to high pore-fluid pressures.

The main conclusions are that *P*-waves show little observable changes before and after the CO_2 injection and significant pore-fluid pressure increases cause the differential opening of low aspect-ratio cracks which leads to decreases in all body wave velocities. The shear-wave velocities decrease differentially and a significant increase in the degree of velocity anisotropy is observed. The saturation change of injecting CO_2 into the reservoir interval has little effect on the effective elastic properties of the fluid-filled material, even though the compressibility of the CO_2 is an order of magnitude smaller than the compressibility of the reservoir fluid.

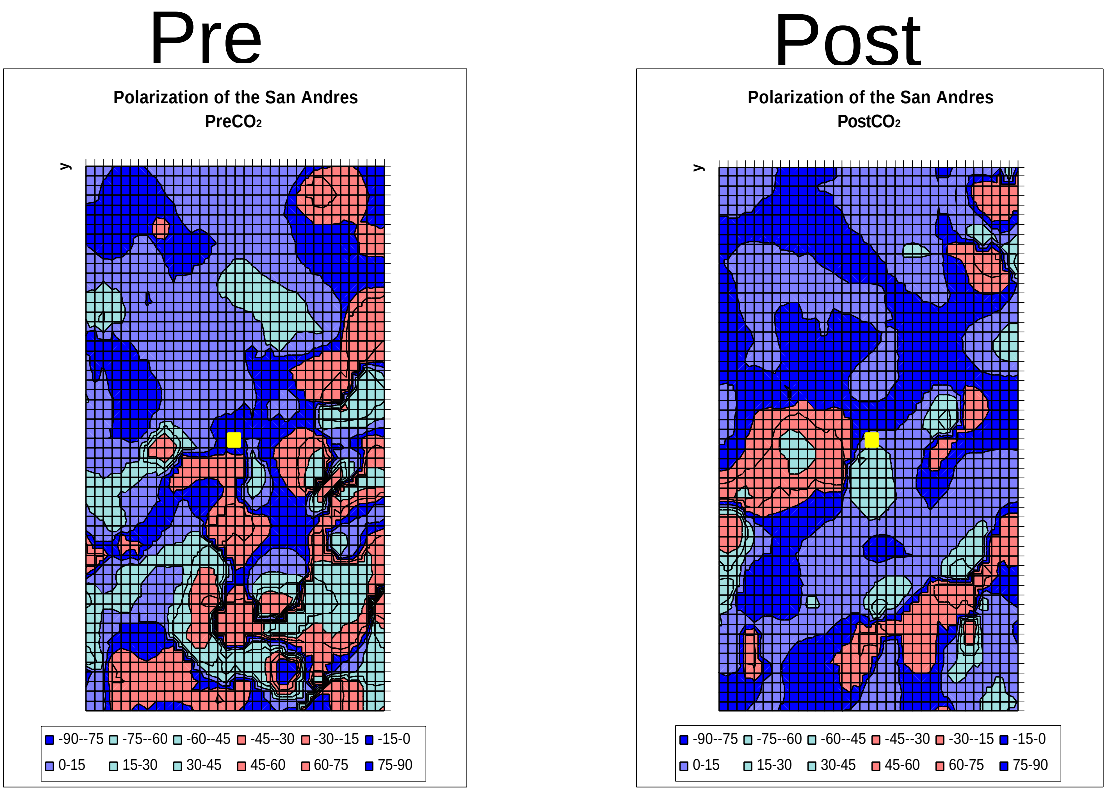

Figure 5.6 Plan view of shear-wave polarisations of the San Andres interval (dolomite) before and after CO_2 injections over a period of two months. Values are in degrees and relative to the natural co-ordinate system 118^o-20^o. The CO_2 injection wells (yellow) are indicated. Each grid point is one CMP location (after Angerer, 2001).

6. Azimuthal attribute analysis of 3D *P*-wave data

In this section, we briefly review the latest progress in using *P*-wave data (azimuthal attribute analysis) for evaluating natural fractures. Acquisition and process of multicomponent shear-wave data are more expensive than *P*-wave data, and for this reason, it is natural to consider whether *P*-waves can be utilised to extract information about natural fractures. Since 1994, the estimation of fracture parameters from azimuthal *P*-wave data has become popular, particularly with 3D *P*-wave data acquired on land. The idea is based on the fact that *P*-waves show azimuthal variations in propagation attributes, i.e. velocity, reflectivity, frequency, as a function of rock properties, such as fracture-induced seismic anisotropy. Assuming the fracture population consists of predominantly one major orientation, Li (1999); Grechka and Tsvankin (1998); Rüger (1998), and others have shown that *P*-wave seismic attributes, such as travel time, interval velocity, reflected wave amplitudes, etc. can be approximately described by an ellipse (Figure 6.1). The long axis of the ellipse indicates the fracture orientation, and the relative ratio of the long to short axes of this ellipse is proportional to the fracture density or intensity of the rock concerned. As we know, at least three data points are required to define an ellipse in azimuthal planes. Thus

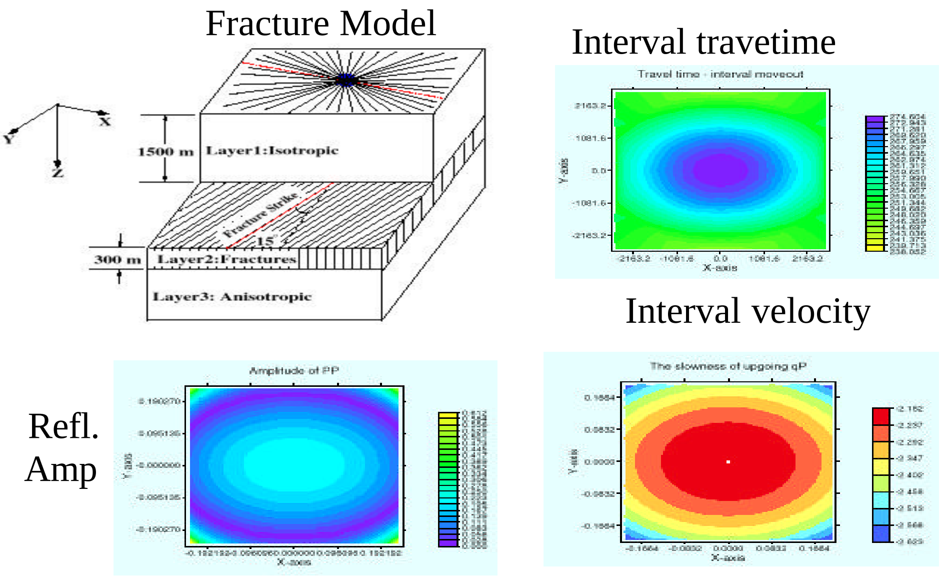

Figure 6.1 Schematic diagram showing the azimuthal response of reflected *P*-waves in fractured rock.

fracture orientation and intensity maps can be built from 3D *P*-wave data if there is sufficient azimuth coverage. Give the limited number of three way intersection points, a simplification of two-way intersection points may be used for mapping relative variation in fracture intensity. This is because *P*-waves typically travel more slowly across fractures than parallel to them. Therefore fractures impart anisotropy to *P*-wave propagation. Such velocity anisotropy is measured as the fractional difference between wave speeds in orthogonal fast and slow directions (two-way intersecting points). Thus an anisotropy (velocity) map may be interpreted in terms of variation of fracture intensity. Among these attributes, reflectivity, in particular, depends on the presence pore contents: changes in impedance. However, true relative amplitudes require careful preservation and processing of the original seismic signals.

In general, *P*-wave attribute variation with azimuth and offset is an emerging tool for azimuthal anisotropy study (MacBeth and Li 1999; Rüger 1998; Rüger and Tsvankin 1997). *P*-wave based technique has been given various names, azimuthal AVO, AVOA, AVAZ, etc. which are very confusing, and we prefer to call it AVD, which stands for *Attribute Variation with Directions* (including azimuths and offsets). It has been reported that azimuthal *P*-wave AVO response can be directly related to gas-filled fractures, and that AVO response measured on seismic line, perpendicular to the strike of gas-filled fractures, can be an order of magnitude greater than AVO response measured in the fracture-parallel direction (Bates et al. 2001).

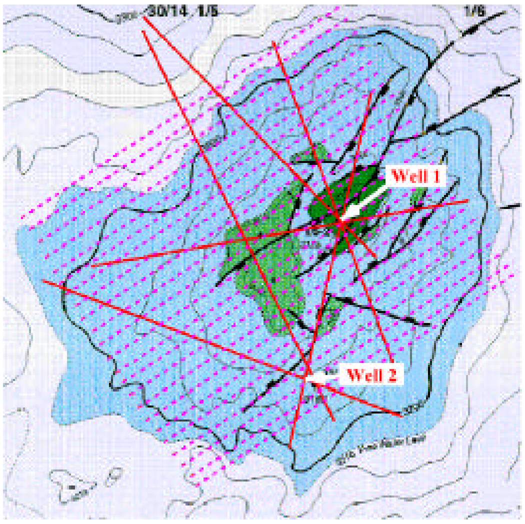

Figure 6.2. Acquisition survey lines of 2D streamer lines on top of a 3D marine streamer survey in a Central North Sea reservoir.

There have been several convincing examples that demonstrate the potential of the AVD technique in land-based 3D seismic data (e.g. Lynn et al. 1996; Bates et al. 2001), but there are very few examples that we know from offshore. Examples given by Liu *et al.* (1999); MacBeth *et al.* (1999); and Smith and McGarrity (2001) from the North Sea are among best ones that we know in the literature.

The application of *P*-wave AVD analysis to marine 3D streamer data is still facing a problem because of the lack of good azimuthal coverage (Liu et al. 1999; Smith and McGarrity 2001). Marine 3D streamer data are usually recorded in a different way from land 3D data, with streamers parallel to each other, giving rise to a very narrow azimuthal coverage. This limits the application of *P*-wave AVD analysis

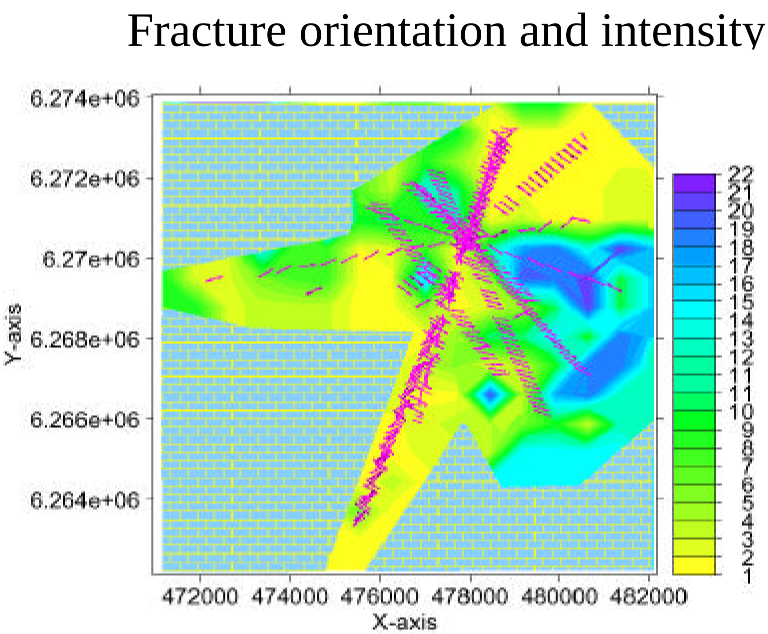

Figure 6.3. Seismic anisotropy map at the reservoir intervals with 2D seismic data lines superimposed. The bars in each lines indicated measured fracture orientations and the colour scales represent the relative percentage of anisotropy that can be interpreted as the spatial distribution intensity of open fractures.

for detecting fractures. One way to compensate for this lack of azimuthal coverage is to combine super-gathers of 3D multi-streamer surveys and crossed 2D lines from other vintage surveys. An recent example that we have been working on is given in Figure 6.2. In this example, at least three-azimuthal gathers can be formed along each CDP point crossing each 2D line. At each 2D and 3D line intersection point, an estimate of ellipticity and orientation was computed from the 'best-fit' velocity and amplitude ellipses implied by the 2D velocity and amplitude functions. In this way, it is possible to obtain fracture orientations from azimuthal AVO analysis, and the estimated fracture orientations along all the 2D lines are shown in Figure 6.3.

Smith and McGarrity (2001) give another good example of using the velocity anisotropy map constructed from two azimuths. They combine a 3D dataset and two 2D lines to form a super-gather and fracture information can then be extracted along 2D lines in the Clair field in the west of Shetland on the UK continental shelf. Their results are in agreement with the results obtained from 3D VSPs. Bates et al. (2001) recently pointed out that if fracture orientations are known, e.g. from stress measurements, it is possible to use two azimuths to estimate the lateral distribution of fracture intensity.

The main benefits of using *P*-waves to characterise fractured reservoirs are

- It is cheaper to acquire and to process the data than multicomponent or OBC data;
- Data are readily available;
- Provide a good start point for a feasibility study using existing data.

However, the main disadvantages are

- Data quality is variable in legacy data;
- Normal marine towed streamer data do not have enough azimuthal coverage;
- Fracture information obtained from *P*-waves is not as reliable as shear-waves.

7. Multicomponent seismic data acquisition and cost issue

Clearly, from the examples in Sections 4 and 5, multicomponent seismic monitoring can provide valuable information about saturation and pore pressure changes during the CO_2 injection. Table 7.1 shows the pros and cons of TLSM (taken from Wang 2000). It is noted that this table is primarily prepared with oil/gas reservoir monitoring in mind, but it should also be applicable for CO_2 injection at the Sleipner Field. In this section, we shall discuss data acquisition geometries and the cost issues.

Table 7.1 Time-lapse seismic monitoring: pros and cons (after Wang 2000)

Favorable factors	Unfavorable factors
• Gaining wide acceptance • Successful trials • Large potential for improved field management • High cost for wells (offshore) • Decreasing cost for 3D survey • Ever increasing computing power • Shortened cycle time • Moderate to good oil price • Integrated, team-based approach	• Too much focus on water flood monitoring which carries higher risk • Not enough risk evaluation or feasibility study - just do it *versus* careful studies • Economic values yet to be proven (except some thermal EOR monitoring projects)

7.1 Data acquisition

We suggest that MC-TLSM can provide a good opportunity for the monitoring of CO_2 storage. Conventional marine 3D streamer data are now routinely acquired, and the data processing and interpretations have matured. When shear-wave information is required, as demonstrated in the last two sections, marine 3D streamer data are clearly not sufficient (Table 7.2). The following are possible acquisition methods that could be used at Sleipner (we include 3D marine streamer survey here for comparison).

1) *2D or 3D marine streamer survey*. This is the cheapest option, and this technology is now routinely used in the North Sea, Gulf of Mexico and around the world. Conventional marine towed streamers are one-component systems, use only hydrophones, and record only *P*-waves. In this we would look for *P*-wave AVO anomalies both laterally and azimuthally in order to obtain the spatial distribution of CO_2 in the subsurface. The information provided by *P*-wave AVO can pinpoint areas with CO_2 concentration and the CO_2 front. This could be better achieved with 3-D techniques. EAP and other groups/companies have developed advanced techniques to perform azimuthal attribute analysis of 3D *P*-wave data for azimuthal anisotropy. Fracture orientation and spatial distribution of fracture intensity can be successfully mapped. BGS has the capability and the analysis of 20km^2 typical 3D data would cost approximately \$20k to \$30k. Some of the applications can be found in Lynn *et al.* (1996); Bates (2001); Liu *et al.* (2000). However, as discussed elsewhere in this report, it is difficult to extract lithology and fluid information from *P*-wave data alone.

2) *3D OBC survey*. This technology is advancing very fast. Marine 4C seismology places 4-components sensors on the sea floor (one hydrophone, a vertical geophone and two horizontal geophones oriented perpendicular to each other. These are grouped together). The three examples in Section 5 provide some good indications as how 4C OBC data can be utilised. Processing software of OBC 4C data are available and some are developing (EAP is playing a leading role). A typical multicomponent OBC acquisition (say $20km^2$) would cost about $600k to $750k, and processing cost would add another $100k.

3) *3D VSPs.* Three component downhole sensors would be placed in existing wells behind casing. As *S*-waves cannot propagate through water, *P*- to *S*- converted waves at the targets can be used as an effective *S*-wave source (similar to the OBC case). By analysing *S*-wave data from several different azimuths, the direction of faster split *S*-wave polarisation can give the direction of preferred alignment of pore spaces and thus the preferred flow pathways. The time difference between two *S*-waves with orthogonal polarisations can give an estimate of fracture intensity and porosity. (See Horne and MacBeth 1997 for various VSP acquisition geometries). Other borehole acquisitions could also be used, but they have not yet been widely used (Ziolkowski 1999).

4) *Permanent reservoir monitoring system (PRMS).* This is basically the same as (2) above, but a permanent reservoir monitoring system is installed in the monitoring site. Ebrom *et al.* (1998) suggest that with repeated marine streamer and OBC surveys, the repeatability associated with positioning, geometry, receiver coupling, weather conditions, etc. can pose significant barriers to 4D success. This problem should be very much reduced in PRMS. PRMS may sound expensive, but it is noted that the incremental cost of future data acquisitions using PRMS should be lower as number of surveys increases (see Figure 7.1 and discussion in Section 7.2). The crossover may occur 2 or 3 times acquisitions for some surveys, however, in others, it may take much longer.

In all experiments, we suggest that repeat or time-lapse surveys are made over regular intervals (for both short term and long term monitoring). Immediately after the CO_2 injection, it would be necessary to repeat surveys at short regular intervals to monitor the changes of rock properties, and for long term monitoring, it would be useful to repeat these surveys every 3 to 5 years, say.

7.2 Cost issue

There is no doubt that multicomponent seismic acquisition is inherently more expensive than the conventional *P*-wave single component survey, however, its advantages must be weighted against this obstacle. From the 1995 SEG Spring Distinguished Lecture, we have the following excerpt: "*Multicomponent 3D seismology involves the acquisition of seismic data in three orientations at each receiver location; two orthogonal and one vertical. The horizontal components of source and receiver displacements enable the recording of shear-waves, which are a powerful complement to compressional-waves. When three-components of source are used, nine times the data of a conventional P-wave 3D can be recorded at approximately one-third more cost thanks to advancements in today's acquisition and processing systems. The cost effectiveness and power of multicomponent 3D will increase as new systems are developed*." The technology today has significantly advanced since 1995, and the acquisition and processing of multicomponent seismics have become routine in oil industry. For multicomponent seismic surveys on land, after a survey of many companies, Kendal and Davis (1996) concluded that the average cost for 3D 3C data is 1.3 times that of conventional 3D *P*-wave data. For 3D full 9C data, it is roughly 2.3 times the conventional 3D. It must be noted that their survey was carried out five years ago, technology has advanced since then and we are confident that the cost should be lower today.

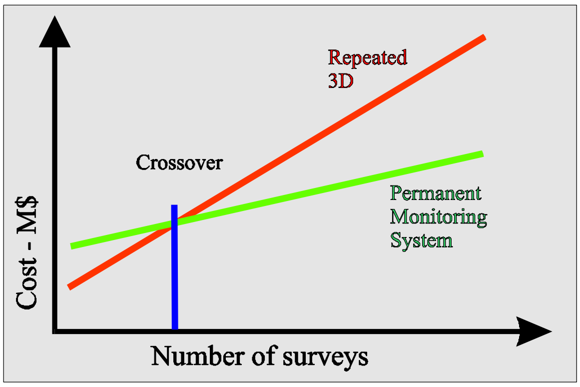

Figure 7.1 Simplifed 4D cost model (adapted Ebrom *et al.* 1998).

For marine OBC surveys, there is no such cost comparison. Marcus Marsh of BP in a recent lecture in Aberdeen (organised by the Aberdeen Formation Evaluation Society on 14 March 2001) suggests that an experimental 4D survey carried in the North Sea over an area of about 390km^2 cost £1.6m, which is about 10% of a horizontal well. Caldwell (1999) suggests that the acquisition of 3D marine multicomponent data is 1.5 to 4 times more expensive than conventional towed streamer 3D, but that is to be expected at this stage of oilfield development. The cost will decrease fairly dramatically as capacity and production rates increase. Figure 7.1, taken from an article in *The Leading Edge* by Ebrom *et al.* (1999), shows a schematic diagram of the cost against number of surveys. Ebrom et al. (1999) suggests that the PRMS (permanent reservoir monitoring system, see Section 7.1) may sound expensive, but it is noted that the incremental cost of future data acquisitions using the PRMS should be lower as number of surveys increases. The crossover may occur 2 to 3 times acquisitions for some surveys, however, in others, it may take much longer. They argue that cost will show no clear increase for permanently installed instruments on the seafloor.

Table 7.2 Comparison of 4 repeated surveys in terms of relative information content (seismic attributes)

	3D streamer	3D OBC	3D VSP	PRMS
P-wave velocity	✓	✓	✓	✓
S-wave velocity		✓	✓	✓
V_p/V_s		✓	✓	✓
Acoustic impedance	✓	✓	✓	✓
Elastic impedance (EI)		✓	✓	✓
Shear EI		✓	✓	✓
P-wave attenuation	✓	✓	✓	✓
S-wave attenuation		✓	✓	✓
Azimuthal variation	✓	✓	✓	✓
S-wave splitting		✓	✓	✓
S-wave polarisation		✓	✓	✓

8. Conclusions

We have used a number of examples in this report to demonstrate the great potential of using multicomponent time-lapse seismic for monitoring fluid migration and associated changes in reservoir properties (saturation and pore pressure) during the CO_2 injection into the Utsira Sand at Sleipner. We summarise here the results of this feasibility study from three viewpoints. The first point is that the Utsira Sand satisfies the criteria to be a ‘good candidate' for time-lapse seismic monitoring. The second point is that multicomponent time-lapse seismic monitoring can help differentiate fluid saturation and pore pressure during the CO_2 injection. The last point is that the MC-TLSM technology is ready for application and all necessary hardware and software tools are available.

8.1 Utsira Sand CO_2 injection at Sleipner Field is suitable for MC-TLSM

Laboratory measurements and theoretical results indicate that seismic monitoring of injected CO_2 is technically viable, and also cost effective for long term monitoring. Experience gained from the application of MC-TLSM technology to oil and gas reservoirs shows that the changes in pore pressure and saturation that are most like to occur during CO_2 injection will cause a large enough changes in seismic properties (velocity, impedance, etc) for successful seismic monitoring. However, not all reservoirs are suitable for such monitoring. Wang (1997) and Jack (1998) suggest that ‘good’ candidate reservoirs suitable for time-lapse seismic monitoring should satisfy some criteria listed in Table 7.1.

Table 8.1 Criteria for good candidate reservoirs for time-lapse monitoring (modified from Wang 1997; Jack 1998)
(1) Reservoirs with weak rocks (2) Reservoirs undergoing large pore fluid compressibility changes (3) Reservoirs undergoing large rock compressibility changes (4) Reservoirs undergoing large temperature changes

These criteria are primarily for oil and gas reservoir monitoring, but they provide a rule of thumb for selecting candidates for time-lapse seismic monitoring. In the context of CO_2 injection into the Utsira Sand at Sleipner, Wang and Jack’s criteria are satisfied. (1) The reservoirs are weak rocks. The Utsira Sand at Sleipner is only about 800 to 1000 m below the seabed and forms a highly porous (about 30% porosity) and permeable sandstone reservoir some 250m thick. (2) A large amount of CO_2 injected into the Utsira Sand will cause large pore fluid compressibility as well as the rock compressibility changes due to changes in effective pore pressure. MC-TLSM technology should be ideal to ensure the success of the SACS2 project.

8.2 MC-TLSM is essential for differentiating changes in saturation and pore pressure

In time-lapse seismic, we measure differences in various seismic attributes. These attributes can then be quantitatively interpreted in terms of physical changes. From the crude analysis presented in Table 8.2, it is clearly seen that *S*-wave attributes are more sensitive to pore pressure change than *P*-wave attributes, whereas *P*-wave attributes are more sensitive to fluid saturation than *S*-waves. Of course, the sensitivity of rock properties will depend on rock type, stress, frequency and other in situ conditions. Caldwell (1999) suggests that anisotropy is also a very important consideration for converted shear-waves rather than for *P*-waves, and industry is rapidly coming to the conclusion that anisotropy must be dealt with. But nevertheless from Table 8.2 we can see there is clearly a need to use shear-wave data through multicomponent data acquisition.

Table 8.2 Sensitivity of seismic attributes to rock properties(1)
(0 = not sensitive, 5 = very sensitive)

Seismic attributes	Fluid saturation	Pore pressure	Stress/fractures & permeability
P-wave velocity	5	5	✓
S-wave velocity(2)	2	5	✓
V_p/V_s	5	4	
Density	5	0	
Acoustic impedance	5	3	✓
Elastic impedance	5	4	✓
Shear elastic impedance	4	4	✓
P-wave amplitude/attenuation	4	5	✓
S-wave amplitude/attenuation	3	5	✓
P-wave AVO response	5	5	✓
PS-wave AVO response	2	5	✓
Azimuthal variation of above (3)	n/a	n/a	✓
Shear-wave splitting (g)	1	5	✓
Shear-wave polarisation	0	5	✓

Note
(1) All these are dependent on rock types, in situ stress, frequency (lab or seismic), etc.
(2) Italics item indicates that this parameter/attribute can only be obtained from shear-wave data.
(3) Azimuthal variation of seismic attributes, e.g. azimuthal AVO or called AVAZ, can be used to map reservoir fractures.

8.3 MC-TLSM technology is ready

The TLSM has advanced greatly in the past five years, particularly since the invention of the 4C OBC acquisition technology. Major oil companies are investing heavily in this technology. BP, for example, suggests 4D seismic monitoring should become routine unless there is a good reason for not doing so. We believe that MC-TLSM technology is now ready for applications.

- *Strong theoretical basis*: Theories have been developed and are now available for quantitative interpretation of multicomponent attributes (e.g. Mavko *et al.* 1998; Hudson 2000; Chapman 2001; Pointer *et al.* 2000, etc.).

- *Extensive laboratory experiments*: The feasibility of time-lapse seismic monitoring based on the laboratory experiments has been studied extensively by many people (e.g. Wang 1997). This provides a strong support for MC-TLSM.

- *Software for data processing*: BGS through EAP among with many other groups and companies have been very active in developing special software for processing multicomponent seismic data since later 1980s. Software for processing 4C OBC data is now also on the market. Special software for isolated changes in time-lapse seismic data and for quantitatively interpreting these changes in rock physical properties are also available.

We are confident that quantitative monitoring of CO_2 injection has a strong physical basis, and experience learnt from the oil/gas sector, including examples in Section 5, has clearly favoured the repeated survey using OBC-based PRSM technology as described in Section 7. The case study in Section 5.4 taken from Angerer (2001) strongly supports our argument that shear-wave based MC-TLSM technology provides the best way to monitor and manage dynamic response of reservoir fluid and pore pressure changes during the CO_2 injection. The success of matching observed changes in time-lapse seismic signature with synthetic seismograms based on poroelastic models that incorporate saturation and pressure changes demonstrates that changes of reservoir properties can be quantitatively predicted. In summary, multicomponent seismic monitoring is not only technically viable, but also cost effective for long term monitoring.

Acknowledgements

Many people have contributed to the idea and results presented in this report, and we have many fruitful discussions with our colleagues Mark Chapman and Hengchang Dai and our students. John Queen's (Conoco) expertise in geophysical characterisation of natural fractures and Stuart Crampin's (University of Edinburgh) experience in seismic anisotropy/shear-waves are always inspiring. John Hudson and Simon Tod (University of Cambridge) are always there when we have a mathematical problem. The authors would like to thank our manager Nick Riley for detailed comments, and particularly Erika Angerer of (formerly) University of Edinburgh (now at WesternGeco) for permission to use some figures from her PhD thesis in this report before she publishes them in her name. The following people provide figures from their work: Erika Angerer (Figures 4.2, 5.5, and 5.6); Mark Chapman (Figures 4.3, and 4.4, formerly at University of Edinburgh, now at BGS); Hengchang Dai (Figure 5.4); Steve Horne (Figure 3.3, formerly at BGS and now at WestGeco); Jerry Yuan (Figure 5.1**,** formerly at BGS, now at PGS); and Yi-Jie Liu (Figures 7.1, 7.2 and 7.3).

In response to the industry need, the Edinburgh Anisotropy Project (EAP) at the British Geological Survey was established in 1988. EAP, currently in its 5th phase programme and sponsored by 13 oil and service companies, has been in the forefront in developing advanced techniques for processing and interpretation of multicomponent seismic data (including 4C OBC data). We thank all sponsors of the EAP for their continuous support.

This work is supported by SACS2 Project No. T-124.167-02, and is published with approval of the Executive Director of the British Geological Survey (NERC).

Appendix A: Seismic anisotropy

Anisotropy is defined to be the '*variation of a physical property depending on the direction in which it is measured.*' (Sheriff 1984). Such variations arise in composite materials when some kind of directional ordering of the components is apparent. In its most fundamental form anisotropy can arise within crystalline lattices such as calcite. However, anisotropy will be observed for any directionally ordering composite materials when observed at appropriate wavelenths. This concept is known as the equivalent medium response and allows such directionally ordering composite materials to be considered as a homogeneous material with an equivalent set of physical properties.

In seismology various mechanisms can lead to anisotropic effects. Perhaps the most obvious cause of seismic anisotropy can occur through the depositional layering of materials with different mechanical properties. Other mechanisms include crack/fracture induced anisotropy, depositional fabrics, aligned pore space, ophitic textures, basaltic layering. Of these crack/fractures induced anisotropy is currently exciting much interest in the geophysical community because of its connection to permeability anisotropy.

Seismic anisotropy leads not only to directional velocity variations but also to the general existence of an additional wave mode. Thus in anisotropic media, three body waves can generally exist with velocities and polarisations determined by the propagation direction. These body waves are referred to as *qP* (quasi-compressional) and *qS1* and *qS2* (quasi-shear) waves. This leads to the phenomenon known as shear-wave splitting or shear-wave birefringence. Since the two shear-waves generally propagate with different velocities and polariations a time delay accumulates which is proportional to the 'strength' of degree of anisotropy and the distance travelled. Shear-wave birefringence is often quantified in terms of this time delay and also the polarisation direction of the leading shear-waves.

The degree of anisotropy is normally measured using three anisotropic parameters introduced by Thomsen (1986):

$$e = \frac{c_{11} - c_{33}}{2c_{33}} \approx \frac{V_p^{//} - V_P^{\perp}}{V_p^{//}}$$ Degree of *P*-wave anisotropy

$$g = \frac{c_{66} - c_{44}}{2c_{44}} \approx \frac{V_S^{//} - V_S^{\perp}}{V_S^{//}}$$ Degree of *S*-wave anisotropy

$$d = \frac{(c_{13} + c_{44})^2 - (c_{33} - c_{44})^2}{2c_{33}(c_{33} - c_{44})}$$ Related to anellipticity of *P*- and *SV*-wavefronts

where c_{ij} (i, j = 1, 2, 3) are elastic stiffness (see Liu *et al.* 2000). $V_p^{//}$ and $V_p^{\perp}$ are the velocities of *P*-waves along and perpendicular to the symmetry plane of the anisotropy material, respectively. $V_s^{//}$ and $V_s^{\perp}$ are the velocities of shear-waves along and perpendicular to the symmetry plane of the anisotropy material, respectively.

References

Angerer, E., 2001, *Processing and modelling of time-lapse changes in Vacuum Field, New Mexico*, PhD Thesis, University of Edinburgh.

Angerer, E., Crampin, S., Li, X.Y. and Davis, T.L., 2001, Processing and modelling time-lapse effects of over-pressured fluid-injection in a fractured reservoir, *Geophy.J.Int.*, submitted.

Barr, F. J., 1997, Dual-sensor OBC technology, *The Leading Edge*, **16,** No.1, 45-51.

Bates, C.R., Phillips, D.R., Grimm, R. and Lynn, H., 2001, The seismic evaluation of a naturally fractured tight gas sand reservoir in the Wind River Basin, Wyoming, *Petroleum Geoscience*, **7**, 35-44.

Caldwell, J., 1999, Marine multicomponent seismology, *The Leading Edge*, **18**, 1274-1282.

Chapman, M., 2000, *Modelling the wide-band laboratory response of rock samples to fluid and pressure changes*, PhD thesis, University of Edinburgh.

Chapman, M., 2001, The dynamic fluid substitution, 71st *SEG Expanded Abstract*, submitted.

Connolly, P., 1999, Elastic impedance, *The Leading Edge*, **18**, No.4, 438-452.

Crampin, S., 1990, The potential of shear-wave VSPs for monitoring recovery, *The Leading Edge,*, **9,** No. 3, 50-52.

Crampin, S., Zatsepin, S.V., Slater, C. and Brodov, L.Y., 1996, Abnormal shear-wave polarisations as indicators of pressures and over pressures, *58th Conf. EAGE, Amsterdam, Extended Abstracts*, X038.

Dai, H.C. and Li, X.Y., 2001, Compensation for the effects of gas clouds on C-wave images – a case stuy from Valhall, *The Leading Edge*, in press.

Davis T.L., Benson R.D., Roche S.L., Talley D., 1997, 4-D 3-C seismology and dynamic reservoir characterization - a geophysical renaissance, *67th Ann. Int. SEG Meeting, Dallas, Expanded Abstracts 1997*, **1,** 880-882.

Duerrast, H. and Siegesmund, S., 1999, Correlation between rock fabrics and physical properties of carbonate rocks, *Int. J. Earth Sciences*, **88**, 392-408.

Duffaut, K., Alsos, T., Landrø, M., Rognø, H. and Al-Najjar, N.F., 2000, Shear-wave elastic impedance, *The Leading Edge*, **19**, No. 11, 1222-1229.

Ebrom, D., 1999, Permanently instrumented offshore oilfields: opportunities and challenges, *Annual Meeting Abstracts, Society Of Exploration Geophysicists*, 1986-1987.

Ebrom, D., Krail, P., Ridyard, D. and Scott, L., 1998, 4-C/4-D at Teal South, *The Leading Edge*, **17,** No.10, 1450-1453.

Endres, A.L. and Knight, R.J., 1997, Incorporating pore geometry and fluid pressure communication into modelling the elastic behaviour of porous rocks, *Geophysics*, **62**, 106-117.

Grechka, V. and Tsvankin, I., 1998, 3-D description of normal moveout in anisotropic inhomogeneous media, *Geophysics*, **63,** No.3, 1079-1092.

Gassmann, F., 1951, Elastic waves through a packing of spheres, *Geophysics*, **16,** No.4, 673-685.

Guest, S., van der Kolk, C. and Potters, H., 1998, The effect of fracture filling fluids on shear-wave propagation, *68th Ann.Int.Mtg., Soc.Exp.Geophys., Exp.Abs.*, 948-951.

Hanson, R., MacLeod, M., Bell, C., Thompson, C. and Somod, J., 1999, Multicomponent Seismic Interpretation - Data Integration Issues, Alba Field, North Sea, *61st Mtg. Eur. Assoc. Expl Geophys., Extended Abstracts, European Association Of Geophysical Exploration, Session:6027.*

Holloway, S. *et al.*, 1996, Joule II Project No. CT92-0031 – Summary Report, *British Geological Survey, Keyworth, UK (Series No. unknown).*
Horne, S., 1995, *Application of genetic algorithms to problems in seismic anisotropy,* PhD Thesis, University of Edinburgh.
Horne, S. and MacBeth, C., 1997, Characterisation of the Fleming Hall Fault Zone using multicomponent VSPs: feasibility and proposed design, *British Geological Survey Technical Report WL/97/1C*, 26pp.
Hudson, J.A., 2000, The effect of fluid pressure on wave speeds in a cracked solid, *Geophys. J. Int.*, **143**, 302-310.
Hudson, J.A., Liu, E. and Crampin, S., 1996, The mechanical properties of materials with interconnected cracks and pores, *Geophys. J. Int*, **124**, 105-112.
Hudson, J.A. and Liu, E., 1999, Effective elastic properties of heavily faulted structures, *Geophysics*, **64**, 479-485.
Iverson, W.P., Fahmy, B.A. and Smithson, S.B., 1989, V_p/V_s from mode-converted *P-SV* reflections, *Geophysics*, **54**, 843-852.
Kendall, R.R. and Davis, T.L., 1996, The cost of acquiring shear waves, *The Leading Edge*, **15,** No.8, 943-944.
Jack, I., 1998. Time-Lapse Seismic in Reservoir Management, *1998 SEG Distinguished Instructor Short Course.*
Li, X.Y., 1997, Fracture reservoir delineating using multicomponent seismic data, *Geophysical Prospecting*, **54**, 39-64.
Li, X., 1999, Fracture detection using azimuthal variation of P-wave moveout from orthogonal seismic survey lines, *Geophysics*, **64,** No.4, 1193-1201.
Li, X.Y. and Mueller, M.C., 1997, Case study of multicomponent seismic data for fracture delineation: Austin Chalk Example, In Marfurt, K. and Palaz, I., (Eds), *Carbonate Seismology*, SEG Special Publication, 337-372.
Li, X.Y., Yuan, J., Ziolkowski, A. and Strijbo, F., 1999, Estimating V_p/V_s ratio from converted waves: a 4C case example, Extended Abstract, *61st Annual International EAGE Meeting, Helsinki, Finland, 7 - 11, June 1999* (4pp).
Liu, E., Crampin, S. and Queen, J.H., 1991, Fracture detection using crosshole surveys and reverse vertical seismic profiles at the Conoco Borehole Test Facility, Oklahoma *Geophys. J. Int*., **107**, 449-463
Liu, E., Crampin, S. and Hudson, J. A., 1997, Diffraction of seismic wave by cracks with application to hydraulic fracturing, *Geophysics*, 1997, **62**, 253-265
Liu, E. and Li, X.Y., 2001, Effects of fluid saturation and pore pressure on seismic anisotropy, *71st Ann. Int. Mtg. Soc. Explor. Geophys., Expanded Abstract, submitted*
Liu, E., Hudson, J.A., and Pointer, T., 2000, Equivalent medium representation of fractured rock, *J. Geophys. Res*., **105**, 2981-3000.
Liu, E., Li, X.Y. and Queen, J. H., 2000, Discrimination of of pore fluids from *P*- and converted shear-waves, *Proc. 9IWSA, Soc. Explor. Soc. (*www.seg.org/9iwsa).
Liu, E. and Li, X.Y., 2001, Sensitivity of interfacial compliances to pore and fracture filling fluids, *Geophysics*, Proc. Workshop on Seismic Signature of Fluid Transport.
Liu, Y., Li, X., MacBeth, C. and Anderton, P., 1999, Analysis of azimuthal variation in P-wave signature from orthogonal streamer lines: *Annual Meeting Abstracts, Society Of Exploration Geophysicists*, 1959-1962.
Liu, Y.J., Li, X.Y. and Anderton, P., 2000, Can we extract fracture information from 3D marine streamer data?, *Expanded Abstract, 70th Ann.Int. SEG Meeting, Calgary*, 4pp.

Lynn, H., Simon, K.M. and Bates, C.R., 1996, Correlation betweeen *P*-wave AVOA and *S*-wave traveltime anisotropy in a naturally fractured gas reservoir, *The Leading Edge*, **15**, 931-936.

Majer, E.L., Datta-Gupta, A., Peterson, J.E., Vasco, D.W., Myer, L.R., Daley, T.M., Kaelin, B., Queen, J.H., d'Onfro, P.S., Rizer, W.D., Cox, D. and Sinton, J., 1996, Utilising crosswell, single well and pressure transient tests for characterising fractured gas reservoirs, *The Leading Edge*, **15,** No.8, 951-956.

MacLeod, M. K., R.A.Hanson, Bell, C. R. and McHugo, S., 1999, The Alba Field ocean bottom cable seismic survey: Impact on development, *The Leading Edge*, **18,** no. 11, 1306-1312.

MacBeth, C., 1995, How can anisotropy be used for reservoir characterization?, *First Break*, **13**, 31-37.

MacBeth, C., Jakubowicz, H., Kirk, W., Li, X.Y. and Ohlsen, F., 1999, Fracture-related amplitude variations with offset and azimuth in marine seismic data, *First Break*, **17**, No.1, 13-26.

MacBeth, C. and Li, X., 1999, AVD -- An emerging new marine technology for reservoir characterization: Acquisition and application, *Geophysics*, **64,** No.4, 1153-1159.

Mavko, G., Mukerji, T. and Dvokin, J., 1998, *The Rock physics handbook*, Cambridge University Press.

Nur, A., 1989, Four-dimensional seismology and (true) direct detectionof hydrocarbons: The petrophysical basis, *The Leading Edge*, **8**, No. 9, 30-36.

Pointer, T., Liu, E., and Hudson, J.A., 2000, Seismic wave propagation in cracked porous media, *Geophys. J. Int*, **142**, 199-231.

Rai, C.S. and Hanson, K.E. 1988, Shear-wave velocity anisotropy in sedimentary rocks: A laboratory study, *Geophysics*, **53**, 800-806.

Robertson, J.D., 1987, Carbonate porosity from *S/P* traveltime ratios, *Geophysics*, **52**, 1346-1354.

Rogers, S., 2001, Stress-related flow: are we looking the right way? *Dialog, published in LPS WebPage (www.lps.org.uk/dialogweb).*

Rüger, A., 1998, Variation of P-wave reflectivity with offset and azimuth in anisotropic media, *Geophysics*, **63,** No.3, 935-947.

Rüger, A. and Tsvankin, I., 1997, Using AVO for fracture detection: Analytic basis and practical solutions, *The Leading Edge*, **16,** No.10, 1429-1430,1432-1434.

Tatham, R.H., 1982, V_p/V_s and lithology, *Geophysics*, **47**, 336-344.

Thomsen, L., 1986, Weak elastic anisotropy, *Geophysics*, **51**, 1954-1966.

Thomsen, L., 1995, Elastic anisotropy due to aligned cracks on porous rock, *Geophys. Prosp.*, **43,** No.6, 805-829.

Thomsen, L., Barkved, O.I., Haggard, B., Kommedal, J.H. and Rosland, B., 1997, Converted wave imaging of Valhall reservoir, *Extended Abstract, 59th EAGE Ann. Int. Conf., Geneva*, Baper No. B048.

Tod, S., Hudson, J.A. and Liu, E., 2001, Pressure induced anisotropy of interconnected cracks, *71st Ann. Int. Mtg. Soc. Explor. Geophys., Expanded Abstract, submitted*.

Sayers, C.M., Johnson, G.M. and Denyer, G., 2000, Pore pressure prediction from seismic tomography, *Presented at OTC 2000 Conference*, No. 11984, 1-7.

Sheriff, R.E., 1984, *Encyclopedic dictionary of exploration geophysics*, 2nd Edition, Society of Exploration Geophysicists.

Smith, R.L. and McGarrity, J.P., 2001, Cracking the fractures – seismic anisotropy in an offshore reservoir, *The Leading Edge*, **20**, No. 1, 19-26.

Stearn, J.E.F., Castoro, A. and Backhouse, R., 2001, Chestnut well planning using elastic impedance of 4C seismic data, *EAGE Expanded Abstract*, 4pp.

Vernik, L. and Liu, X., 1997, Velocity anisotropy in shales: A petrophysical study, *Geophysics*, **62**, 521-532.

Wang, Z., 1997, Feasibility of time-lapse seismic reservoir monitoring: The physical basis, *The Leading Edge*, **16,** No.9, 1327-1329.

Wang, Z., 2000, 4D seismology: the technology, applications, and challenges, *presented at SEG Reservoir Geophysics Symposium, Shenzhen, China (PowerPoint file).*

Wang, Z., Cates. M.E. and Langan, R.T. 1998. Seismic monitoring of a CO_2 flood in a carbonate reservoir: A rock physics study, *Geophysics*, **63**, 1604-1617.

Winterstein, D.F. and Meadows, M.A., 1991. Shear-wave polarisation and subsurface stress directions at Lost Hill Field, *Geophysics*, **56**, 1331-1348.

Zatsepin, S.V. and Crampin, S., 1997. Modelling the compliance of crustal rock - I. Response of shear-wave splitting to differential stress, *Geophys. J. Int*., **129**, 477-494.

Xu, S. and White, R.E., 1995, A new velocity for clay-sand mixtures, *Geophys. Prosp*., **43,** No.1, 91-118.

Yan, J., Liu, E., Li, X.Y., and Scrutton, R., 2001, Petrophysical inversion of well-log and VSP data using a dual-prosity model, to be presented at 63rd EAGE Meeting, Amsterdam.

Yuan, J., Li, X.Y. and Ziolkowski, A., 1999, Anisotropy and correlation analysis in North Sea 4-C sea-floor seismic data, Extended Abstract, *61st Annual International EAGE Meeting, Helsinki, Finland, 7 - 11, June 1999* (4pp).

Ziolkowski, A., 1999, Multiwell imaging of reservoir fluids, *The Leading Edge*, **18,** No.12, 1371-1373, 1376.